Insertion of N-terminal hinge glycosylation enhances interactions of the fragment crystallizable (Fc) region of human IgG1 monomers to glycan-dependent receptors and blocks hemagglutination by the influenza virus

Patricia A. Blundell[§], Dongli Lu*, Mark Wilkinson[§], Anne Dell*, Stuart Haslam* and Richard J. Pleass[§1]

From the [§]Department of Parasitology, Liverpool School of Tropical Medicine, Liverpool, L3 5QA, United Kingdom.

*Department of Life Sciences, Imperial College London, London, SW7 2AZ, United Kingdom.

Running title: Engineering IgG1-Fc monomers for enhanced receptor interactions

Key words: IgG, immunoglobulin, Fc-receptors, lectin, glycan, sialic acid, sialylation, siglec, C-type lectin, Fc-multimers, Fc-monomers, IVIG, complement, influenza virus, agglutination

[1.] To whom correspondence should be addressed: Dept. of Parasitology, Liverpool School of Tropical Medicine, Pembroke Place, Liverpool, L3 5QA, United Kingdom. Tel: 44-151-345-7793; E-mail: richard.pleass@lstmed.ac.uk

[2.] The abbreviations used are: Fc, Fragment crystallizable; IVIG, Intravenous Immunoglobulin; ITP, Idiopathic Thrombocytopenic Purpura; tp, tailpiece; Siglec, Sialic acid-binding immunoglobulin-type lectin; CD, Cluster Designation; DC-SIGN, Dendritic Cell-Specific Intercellular Adhesion Molecule-3-grabbing Non-Integrin; DCIR, C-type Lectin Dendritic Cell Immunoreceptor; CLEC, C-type Lectin; HA, Hemagglutinin; MBL, Mannose-Binding Lectin; MMR, Macrophage Mannose Receptor; mAbs, monoclonal Antibody; MALDI, matrix-assisted laser desorption ionisation; TOF, time-of-flight; SEC, Size-Exclusion Chromatography; SPR, Surface Plasmon Resonance.

Abstract

In therapeutic applications where the Fc of IgG is critically important, the receptor binding and functional properties of the Fc are lost after de-glycosylation, or removal of the unique Asn[297] N-X-(T/S) sequon. A population of Fcs bearing sialylated glycans has been identified as contributing to this functionality, and high levels of sialylation also lead to longer serum retention times advantageous for therapy. The efficacy of sialylated Fc has generated an incentive to modify the unique N-linked glycosylation site at Asn[297], either through chemical and enzymatic methods or by mutagenesis of the Fc, that disrupts the protein-Asn[297] carbohydrate interface. Here we took an alternative approach, by inserting or deleting N-linked attachment sites into the body of the Fc, to generate a portfolio of mutants with tailored effector functions. For example, we describe mutants with enhanced binding to low-affinity inhibitory human Fcγ and glycan receptors that may be usefully incorporated into existing antibody-engineering approaches to treat or vaccinate against disease. The IgG1 Fc-fragments containing complex sialylated glycans attached to the N-terminal Asn[221] sequon bound influenza virus hemagglutinin and disrupted influenza A-mediated agglutination of human erythrocytes.

Introduction

Multiple lines of evidence have shown that glycosylation is critical to driving either the anti- or pro-inflammatory capability of IgG [1]. Glycosylation of the only available carbohydrate attachment site (Asn^{297}) in the Fc is essential for interactions with type 1 receptors (Fcγ) and type 2 receptors (glycan dependent), but also for driving interactions with the complement cascade [2–5].

In humans, infusion of Fc fragments is sufficient to ameliorate idiopathic thrombocytopenic purpura (ITP) in children, demonstrating the therapeutic utility of the Fc *in vivo* [6]. These anti-inflammatory properties of the Fc are lost after deglycosylation of IgG, and a population of IgG-bearing sialylated Fcs has been identified as making a significant contribution to the control of inflammation in animal models [7, 8]. Higher levels of sialylation also leads to longer serum retention times [9, 10], and studies in humans and mice have shown that influx and efflux of IgG into the central nervous system (CNS) is glycan and sialic acid dependent [11–16].

Consequently, the efficacy of sialylated Fc has generated an incentive to modify the existing glycans on Asn^{297}, either by chemical means or through mutagenesis programs in the Fc protein backbone that disrupt the protein-Asn^{297}-carbohydrate interface [17–19]. However, chemical modification of pre-existing glycans is expensive and reliant on a sustainable source of human Fc, while mutagenesis approaches on the Fc, or expression in glycosidase-deficient/transgenic cell lines, have yielded little improvement in Asn^{297} sialylation to the levels required for significant enhancements in the affinity of binding to FcγRs [18, 19]. Recently, co-administration of two glycosyltransferase Fc-fusion proteins has been shown to convert endogenous IgG into sialylated anti-inflammatory IgGs that attenuate autoimmune disease in animal models in a platelet-dependent manner [20].

Although *in vivo* enzymatic sialylation may circumvent many technical issues concerned with chemical or mutagenic approaches to generating sialylated IgG, it may not be appropriate in all clinical settings for example in neurological diseases (e.g. neuromyelitis optica), where the target site is mostly devoid of platelets, and where two different Fc fusions would need to

3

117 traverse the blood-brain barrier simultaneously. This approach also runs the

118 risk of off-target glycan modifications and known immunogenicity of long-term

119 administration of Fc fusions (21).

120   Mutagenesis studies to date have also been limited in two further

121 respects. Side-chain changes have typically been restricted to alanine or

122 serine, and, functionality studies have mostly been confined to FcγR binding

123 studies (22, 23). It is therefore of academic interest and potential clinical value

124 to explore more thoroughly how the introduction of additional N-glycan sites

125 into the Fc might affect changes in binding to FcγR and other atypical Fc-

126 glycan receptors, including Siglecs and C-type lectins.

127   We recently published two complementary approaches that radically

128 increase the sialic acid content of the Fc (24), first by insertion of the 18

129 amino-acid tailpiece (tp) from IgM onto the C-terminus of the IgG1-Fc into

130 which a cysteine-to-alanine substitution is made at Cys^{575}, and secondly by

131 the addition of an extra N-glycan to the N-terminus at position Asn^{221}. This

132 approach resulted in both multimeric and monomeric molecules that are

133 >75% sialylated (compared to 2% for the IgG-Fc control) that bind to sialic

134 acid-dependent receptors, including Siglec-1 and myelin-associated

135 glycoprotein (MAG) (24), which are clinically implicated in the control of

136 neuropathology (25, 26). As many pathogens rely on glycans to infect host

137 cells, these reagents may also be useful as inhibitors of infection (27).

138   The human IgG1-Fc typically does not bind glycan receptors because

139 the glycan attached to Asn^{297} is largely buried within the cavity formed by the

140 CH2-CH3 homodimer (28, 29). The location and content of glycans attached

141 at Asn^{297} also modulates the affinity of the Fc for binding to the classical

142 FcγRs, through conformational changes imparted to the FcγR-binding region

143 located in the lower hinge (30). Here we show that these limitations to Asn^{297}-

144 directed receptor binding can be overcome through a program of mutagenesis

145 aimed at disrupting disulfide bonding while enhancing N-linked glycosylation

146 within the IgG1 Fc (Figs. 1, 2).

147   To this end we created two panels of human IgG1 Fc mutants (Figs.

148 1,2) by deleting critical disulfide bonds, and/or by inserting or deleting N-linked

149 asparagine attachment sites located within the previously described IgG1-Fc

150   multimer (2, 5, 24, 31). This approach not only yielded molecules with

151   enhanced binding to low-affinity FcγRs, but also showed interactions with

152   receptors not previously known to bind the IgG1 Fc, including Siglec-1, Siglec-

153   2, Siglec-3, Siglec-4, CD23, Dectin-1, Dectin-2, CLEC-4A (DCIR), CLEC-4D,

154   MMR, MBL and DEC-205. Finally, we were able to identify monomeric Fc

155   glycan mutants with enhanced binding to influenza A virus hemagglutinin (HA)

156   that inhibited viral-mediated agglutination of human erythrocytes.

157

158

159

160

161

162

163

164

165

166

167

168

169

170

171

172

173

174

175

176

177

178

179

180

181

182

Materials and Methods

Production of mutants

The generation of glycan mutants in all combinations has been described previously for the hexa-Fc that contains cysteines at both positions 309 and 575 (24). To make the new mutants described in Fig. 1 in which Cys[575] was mutated to alanine, PCR overlap extension mutagenesis was used with a pair of internal mismatched primers 5'-ACCCTGCTTGCTCAACTCT-3' / 3'-GGCCAGCTAGCTCAGTAGGCGGTGCCAGC-5' for each plasmid vector coding for a designated glycan modification. The parental plasmids used for these new PCR reactions have been described previously (24). The resulting C575A mutants were then further modified to remove Cys[309] using primer pair 5'-TCACCGTCTTGCACCAGGACT-3' / 3'-AGTCCTGGTGCAAGACGGTGA-5' to create the panel of double cysteine knockouts described in Fig. 2. To verify incorporation of the desired mutation and to check for PCR-induced errors, the open reading frames of the new mutants were sequenced on both strands using previously described flanking primers (24). CHO-K1 cells (European Collection of Cell Cultures) were transfected with plasmid using FuGene (Promega), and Fc-secreting cells were cloned, expanded, and the proteins purified as previously described (2, 31).

Receptor and complement binding assays

Methods describing the binding of mutants to tetrameric human DC-SIGN (Elicityl), Siglec-1, Siglec-4, and Siglec-3 (Stratech Scientific) have all been described previously (2, 31). The same ELISA protocol was used for Siglec-2, CD23, dec-1, dec-2, clec-4a, clec-4d, MBL and MMR (Stratech Scientific or Bio-Techne). Binding of C1q and C5b-9 have been described previously (2, 31). ELISAs were used to investigate binding of Fc glycan mutants to human FcγRI, FcγRIIA, FcγRIIB, FcγRIIIA, and FcγRIIIB (Bio-Techne). Receptors were coated down on ELISA plates (Nunc) in carbonate buffer pH 9 (Sigma-Aldrich) at 2 μg/ml overnight at 4°C, unless otherwise specified. The plates were blocked in PBS/0.1% Tween-20 (PBST) containing 5% dried skimmed milk. Plates were washed three times in PBST before adding Fc mutant proteins at the indicated concentrations and left at 4°C overnight. Plates were

6

216   washed as above and incubated for 2h with 1:500 dilution of an alkaline

217   phosphatase-conjugated goat F(ab')$_2$ anti-human IgG (Jackson Laboratories).

218   Binding of the secondary detecting Fab'$_2$ anti-human Fc was checked by

219   direct ELISA to every mutant to ensure there were no potential biases in the

220   detection of binding of different mutants to different receptors (Supplementary

221   Fig S1A). Plates were washed and developed with 100 μl/well of a Sigmafast

222   *p*-nitrophenyl phosphate solution (Sigma-Aldrich). Plates were read at 405nm,

223   and data plotted with GraphPad Prism.

224

225   *Binding to hemagglutinin*

226   ELISA plates were coated with 5 μg/mL recombinant HA from different

227   influenza A and B viruses (BEI Resources) or native influenza A New

228   Caledonia H1N1 virus (2B Scientific) in carbonate buffer pH 9 and left at 4°C

229   overnight. Plates were washed five times with TSM buffer (20 mM Tris-HCl,

230   150 mM NaCl, 2 mM CaCl$_2$, 2 mM MgCl$_2$), prior to blocking for 2h in 150μl per

231   well of TMS buffer containing 5% bovine serum albumin. After washing as

232   before, 100μl of Fc fragments at 30μg/mL in TSM buffer was added in

233   triplicate wells. Fc fragments were allowed to bind overnight at 4°C. Plates

234   were washed five times with excess TSM buffer, prior to the addition of 100μl

235   per well of alkaline-phosphatase conjugated F(ab')$_2$ goat anti-human IgG1

236   Fcγ fragment-specific detection antibody diluted 1 in 500 in TMS buffer.

237   Glycosylated Fc fragments that bound to the glycan receptors were left to bind

238   the conjugated antibody for 1h at room temperature on a rocking platform.

239   Plates were washed as above and developed for 10 minutes with 100μl per

240   well of p-Nitrophenyl phosphate. Plates were read at 405nm using a LT4500

241   microplate absorbance reader (Labtech), and the data plotted with GraphPad

242   Prism.

243

244   *Hemagglutination inhibition assay*

245   To determine the optimal virus-to-erythrocyte ratio, two-fold virus stock (2B

246   Scientific) dilutions were prepared in U-shaped 96-well plates (Thermo

247   Scientific). The same volume of a 1% human O+ red blood cell suspension

248   (Innovative Research) was added to each well and incubated at RT for 60 min

249 until erythrocyte pellets had formed in the negative control. After quantifying

250 the optimal virus-to-erythrocyte concentration (4HA units), serial two-fold

251 dilutions of Fc, control IVIG (GammaGard, Baxter Healthcare) or polyclonal

252 goat anti-influenza H1N1(Biorad) were prepared, starting at a concentration of

253 2μM, and mixed with 50μl of the optimal virus dilution. After a thirty minute

254 incubation at 4°C 50μl of the human erythrocyte suspension was added to all

255 wells and plates incubated at RT for 1h, after which erythrocyte pellets could

256 be observed in the positive controls.

257

258 *N-glycomic analysis*

259 N-glycomic analysis was based on previous developed protocol with some

260 modifications (32). Briefly, the N-glycans from 50μg of each sample were

261 released by incubation with NEB Rapid™ PNGase F and isolated from

262 peptides using Sep-Pak C18 cartridges (Waters). The released N-glycans

263 were permethylated, prior to Matrix-assisted laser desorption ionization

264 (MALDI) MS analysis. Data were acquired using a 4800 MALDI-TOF/TOF

265 mass spectrometer (Applied Biosystems) in the positive ion mode. The data

266 were analyzed using Data Explorer (Applied Biosystems) and

267 Glycoworkbench (33). The proposed assignments for the selected peaks were

268 based on composition together with knowledge of the biosynthetic pathways.

269

270 *Binding to FcγRs by Biacore*

271 Binding to FcγRs was carried out using a Biacore T200 biosensor (GE

272 Healthcare). Recombinantly expressed FcγRs (R&D systems and Sino

273 Biological) were captured via their histidine tags onto CM5 chips pre-coupled

274 with ~9000 RU anti-His antibody (GE Healthcare) using standard amine

275 chemistry. Fc mutants were injected over captured receptors at a flow rate of

276 20 μl/min and association and dissociation monitored over indicated time

277 scales before regeneration with two injections of glycine pH 1.5, and

278 recalibration of the sensor surface with running buffer (10mM HEPES, 150

279 mM NaCl, pH 7.0). Assays were visualized with Biacore T200 evaluation

280 software v 2.0.1.

281

Results

Disulfide bonding and glycosylation influence the multimerization states of hexa-Fc

To determine the contribution of two N-linked glycosylation sites (Asn^{297} and Asn^{563}) and two cysteine residues (Cys^{309} and Cys^{575}) in the multimerization of hexa-Fc (2), we created two panels of glycosylation- and cysteine-deficient mutants by site-directed mutagenesis, using the previously described hexa-Fc as the template (Figs. 1, 2) (2, 24). We also inserted an N-linked attachment site at the N-terminus of the Fc (D221N), to investigate the impact of additional glycosylation on Fc function (Figs. 1, 2). Following transfection of these mutated IgG1-Fc DNAs into CHO-K1 cells, stable clonal cell lines were established, and the secreted Fcs were purified by protein G affinity chromatography. The purified proteins were analyzed by SDS-PAGE (Fig. 3) and SEC-HPLC (Supplemental Figs. S1D).

When analyzed under non-reducing conditions (Fig. 3A, 3C and Supplemental Fig. S1C), the C575A mutant migrated mostly as monomers (~55 kDa), with a very small proportion of dimer (~110 kDa) and trimer (~165 kDa). Insertion of a glycan at Asn^{221} into the C575A mutant (to create D221N/C575A) resulted in reduction of the trimer fraction and a decrease in the proportion of dimers observed, although the molecular weights of each of the species increased as a consequence of the additional N-terminally attached Asn^{221} sugar (Fig. 3A-3C, Supplemental Fig. S1C).

Because we had previously shown that removal of the tailpiece glycan (Asn^{563}) in hexa-Fc led to the formation of dodecamers (24), we reasoned that a similar mutation introduced into the C575A mutants would also lead to enhanced dodecamer formation. Surprisingly, removal of Asn^{563}, as in N563A/C575A, N297A/N563A/C575A, D221N/N563A/C575A and D221N/N297A/N563A/C575A, led to the formation of a laddering pattern of different molecular masses from ~50 to greater than 500 kDa (Fig. 3A, red arrows, 3C), representing monomers, dimers, trimers, tetramers, pentamers, hexamers, etc. Weaker bands between these species may represent 25 kDa folding intermediates that include Fc halfmers (Fig. 3A, blue arrows). All proteins in which the tailpiece Asn^{563} glycan was substituted for alanine run as

9

316   multimers in solution when examined by SEC-HPLC (Supplemental Fig. S1C).

317   By running these mutants under reducing conditions, we were able to

318   determine the relative sizes and occupancy of the glycans attached at each

319   position, showing that the Asn[221] and Asn[563] glycans are larger than that at

320   Asn[297], and that fully aglycosylated null mutants such as

321   N297A/N563A/C575A are ~10 kDa lighter than either hexa-Fc or C575A

322   glycan competent molecules (Fig. 3B).

323   As Cys[309] is present in these mutants (Fig. 1, Fig. 3A-3C), the ladders

324   may arise through disulfide bond formation between the only freely available

325   sulfhydryl at Cys[309] in two adjacent monomers. We reasoned that the loss of

326   the tailpiece glycan in these four N563A mutants allows the hydrophobic

327   amino-acid residues (Val[564], Leu[566] and Ile[567]) also located in the tailpiece to

328   cluster, thereby permitting disulfide bonding at Cys[309].

329   To test the hypothesis that Cys[309] was indeed responsible for the

330   laddering seen with the N563A deficient mutants, we generated a second

331   panel of C575A mutants in which Cys[309]/Leu[310] are mutated to Leu[309]/His[310] as

332   found in the wild-type IgG1 Fc sequence (Fig. 2). We also generated the

333   mutant CL309-310LH (C309L) in which the tailpiece Cys[575] was still present.

334   This mutant ran similarly to hexa-Fc under non-reducing conditions, albeit with

335   the presence of intermediates (Fig. 3D, blue arrows) that were notably absent

336   in hexa-Fc, showing that Cys[309] stabilizes the quaternary structure in the

337   presence of Cys[575].

338   Importantly, the loss of Cys[309] also resulted in the loss of the ladders

339   previously seen in the Cys[309] competent mutants (Fig. 3D, 3F versus 3A, 3C),

340   with all the double cysteine mutants now running principally as monomers by

341   SDS-PAGE. The C309L/N297A/C575A mutant runs as four different

342   monomeric species (Fig. 3D) that resolve as two bands under reduction (Fig.

343   3E). These bands may represent glycan variants arising at Asn[563]. Given that

344   these variants are absent in the C309L/C575A mutant, we conclude that the

345   presence of Asn[297] glycan also controls glycosylation efficiency at Asn[563]. To a

346   degree, the presence of the Asn[221] glycan also limits the occurrence of these

347   Asn[563] glycoforms, as under reduction only a single band is seen in the

348   D221N/C309L/N297A/C575A mutant (Fig. 3E).

349   Although the panel of double cysteine knockouts run mostly as

350 monomers on SDS-PAGE (Fig. 3D, 3F), the double cysteine knockouts

351 containing the N563A substitution run as a mixture of monomers and

352 multimers in solution (Supplemental Fig. S1C). Thus, removal of the bulky

353 Asn^{563} glycan exposes hydrophobic amino acid residues in the tailpiece that

354 facilitate non-covalent interactions in solution that would not otherwise readily

355 occur in the presence of the sugar.

356

357

358 ***The Asn^{297} and Asn^{563} glycans are critical for the interactions of mutants***

359 ***with glycan receptors, and their absence can be compensated by the***

360 ***presence of Asn^{221}***

361   To determine which N-linked glycan in the double cysteine knockout

362 mutants (Fig. 2) contributes to receptor binding, we investigated their

363 interaction with soluble recombinant glycan receptors by ELISA (Fig. 4, Table

364 1). In stark contrast to the IgG1-Fc control, mutants in which both Asn^{297} and

365 Asn^{563} are present (e.g. C309L/C575A) bound all twelve glycan receptors

366 investigated (Fig. 4). Removal of the tailpiece glycan Asn^{563}, as in

367 C309L/N563A/C575A or C309L/N297A/N563A/C575A, abolished binding to

368 these same receptors, showing that Asn^{563} is required for glycan-receptor

369 binding.

370   Removal of the glycan at Asn^{297}, as in C309L/N297A/C575A, also

371 abolished binding to all glycan receptors with the exception of Siglec-1. Taken

372 together, the data shows that both Asn^{563} and Asn^{297} are required for the

373 broad glycan-receptor binding seen with the C309L/C575A mutant (Fig. 4 and

374 Table 1).

375   With the exception of MBL, MMR and DC-SIGN, binding by the double

376 aglycosylated knockout C309L/N297A/N563A/C575A could be reinstated by

377 the addition of sialylated glycans at Asn^{221}, creating the mutant

378 D221N/C309L/N297A/N563A/C575A. The Asn^{221} glycan contributes all the

379 sialylated sugars that are required to explain the marked improvements in

380 binding to other glycan receptors, compared to all equivalent mutants lacking

381 Asn^{221} (Supplemental Figs. S2-S4). This is in agreement with our previous

382 work where we demonstrated in fully cysteine-competent multimers that

383 Asn^{221} is >75% terminally sialylated (24).

384   The C309L mutant that can form cysteine-linked multimers due to the

385   retention of Cys[575] in the tailpiece (Figs. 3D, 3F and supplemental Fig. S1C),

386   was unable to bind to any glycan receptors with the exception of CD23 (Fig.

387   4). Thus, the Asn[563] glycans are only available for binding when attached to

388   lower valency molecules and are buried within multimers that form either

389   through Cys[309] driven covalent bridging, or, by non-covalent clustering

390   through multiple hydrophobic amino acids located in the tailpiece (e.g.

391   C309L/N563A/C575A).

392   We next investigated binding of the panel of C575A mutants in which

393   Cys[309] is still present (Fig. 1), and that we had shown to have the tendency to

394   form dimers and laddered multimers (Fig. 3A, 3C and Supplemental Figs.

395   S1C). This panel of molecules, in which disulfide bonding mediated by Cys[309]

396   could still occur, bound less well to all the glycan receptors investigated (Fig.

397   5). With the sole exception of Siglec-1, the presence of the Asn[221] glycan was

398   unable to improve binding, in contrast to the double cysteine knockouts. We

399   conclude that N-glycans at all three attachment sites (Asn[221], Asn[297] and

400   Asn[563]) are more predisposed to binding to glycan receptors when expressed

401   on monomers, and that the presence of Asn[221] as the only glycan is sufficient

402   to impart this broad specificity of binding, as exemplified by

403   D221N/N297A/N563A/C575A and D221N/C309L/N297A/N563A/C575A (Figs.

404   4 and 5).

405   We observed that the aglycosylated mutant N297A/N563A/C575A had

406   a propensity to bind glycan-receptors (Fig. 5). We do not have a simple

407   answer for this observation, although the lack of binding by its counterpart

408   C309L/N297A/N563A/C575A in which Cys309 is absent, suggests that it may

409   be glycan independent and a consequence of increased avidity interactions

410   through multimerization (compare Fig. 3A v 3D).

411

412   ***Glycan receptor binding is critically dependent on the presence of N-***

413   ***linked glycans***

414   To be certain that glycan receptor binding was dependent on the presence of

415   N-linked carbohydrates, and more specifically sialic acid, these sugars were

416   removed from the tri-glycan D221N/C309L/C575A mutant using either

417   PNGase F or neuraminidase (Supplemental Fig. S1B). As expected, the

418 D221N/C309L/C575A mutant treated with PNGase F was unable to bind any
419 of the receptors investigated, while treatment with neuraminidase inhibited
420 binding to the sialic acid-dependent receptors (Supplemental Fig. S1B).
421

422 ***Asn[221]-based monomers show differential binding to low-affinity human***
423 ***FcγRs***
424   Given the remarkable binding to glycan receptors seen with some of
425 the glycan-modified mutants, we tested the impact that this extra
426 glycosylation conferred on binding to the classical human FcγRs (Fig. 6, Table
427 2). The presence of Asn[221], for example in the
428 D221N/C309L/N297A/N563A/C575A mutant, imparted improved binding to
429 FcγRIIB (CD32B) even in the absence of both Asn[297] and Asn[563] when
430 compared to the IgG1-Fc, and controls in which Asn[221] was absent (Fig. 6, for
431 FcγRIIB compare filled symbols versus unfilled symbols). However, the
432 presence of Asn[221] did not improve binding to FcγRIIIA (compare
433 D221N/C309L/N563A/C575A and C309L/N563A/C575A), although binding of
434 both mutants was considerably stronger than the IgG1-Fc monomer control
435 (Figs. 6 and 7B). We hypothesize that the enhanced binding observed with
436 the N563A-deficient mutants is a consequence of increased tailpiece-
437 mediated assembly by all the Asn[563] deficient proteins (supplemental Fig.
438 S1C). Improved binding to FcγRI was also observed with these two mutants
439 against the IgG1-Fc control (Figs 6 and 7A), although no improvements were
440 seen with respect to either FcγRIIA or FcγRIIIB for any of the mutants tested.
441   Both the double cysteine knockouts, C309L/N563A/C575A and
442 D221N/C309L/N563A/C575A that form multimers in solution, and bound
443 FcγRI and FcγRIIIA (Val[176]) strongly in ELISAs, were tested for binding FcγRs
444 receptors by surface plasmon resonance analysis (Fig. 7). Both mutants
445 displayed slower apparent off-rates compared with the control Fc monomer,
446 consistent with avidity effects either through binding to multiple immobilized
447 FcγRs molecules or rebinding effects (Fig. 7). The loss of Asn[297] in the
448 C309L/N297A/C575A and D221N/C309L/N297A/C575A mutants resulted in
449 molecules that were unable to bind FcγRs, as previously shown by ELISA
450 (Figs. 6 and 7).

13

451   We next investigated binding of the multimers formed through Cys[309]

452 (Figs. 1, 3A, 3C). In multimers, the presence of Asn[221] reduced binding to all

453 FcγRs (Fig. 6, Table 2), while binding to the glycan receptors, although lower

454 than that seen with monomers, was retained (Fig. 5). Multimers in which

455 Asn[563] and Cys[575] are both mutated to alanine, as in N563A/C575A, bound

456 very strongly to FcγRI and FcγRIIIA, with improved binding to FcγRIIB when

457 compared to either the hexa-Fc or IgG1-Fc controls (Fig. 6). The

458 aglycosylated multimer N297A/N563A/C575A bound very well to the inhibitory

459 FcγRIIB receptor while retaining binding to FcγRI (Fig. 6).

460

461

Asn[221]-based monomers and multimers show reduced complement activation

464   Binding of C1q and activation of the classical complement pathway by

465 complex monomers (Fig. 8A) and multimers (Fig. 8B) was assessed using

466 ELISA and summarized in Table 3 (24, 31). With the exception of

467 D221N/C309L/N563A/C575A, all Asn[221]-containing monomers bound C1q

468 less well than the IgG1-Fc or Asn[221]-deficient controls (Fig. 8A), and all four

469 Asn[221]-containing proteins were unable to activate the classical complement

470 pathway to its terminal components (Fig. 8A). These findings were

471 recapitulated with the Cys[309] mutants (Fig. 8B), including those proteins

472 shown to form multimers (e.g. D221N/N297A/N563A/C575A against

473 N297A/N563A/C575A). As previously shown by other groups, we have

474 identified mutants capable of forming multimers (e.g. C309L and

475 D221N/N563A/C575A) that avidly bound C1q but were unable to fix C5b-9

476 when compared with hexa-Fc (Fig. 8B)(34).

477

Asn[221]-based monomers and multimers exhibit complex sialylation patterns

480   The structure of the N-glycan on the Fc of IgG antibodies has been

481 shown to influence multiple receptor interactions. For example, the interaction

482 of IVIG with glycan receptors has been attributed to direct and/or indirect

483 effects of N-glycan sialic acid on the Fc (30, 35, 36). Therefore, we

484   investigated the nature of the N-glycans on the two panels of glycosylation-

485   and cysteine-deficient mutants by MALDI-TOF mass spectrometry based

486   glycomic analysis (Fig. 9, supplemental Figs. S2-S4).

487   We previously demonstrated that N-glycans from both IgG1-Fc and

488   clinical IVIG preparations are dominated by biantennary complex N-glycans

489   with 0, 1 or 2 galactose residues (37). A minority of these complex structures

490   are also mono-sialylated (2, 23). Representative glycomic data is presented in

491   Figure 9 for N297A/C575A and D221N/N297A/N563A/C575A.

492   In both samples the spectra demonstrate a higher level of N-glycan

493   processing with enhanced levels of biantennary galactosylation and

494   sialylation. In addition, larger tri- and tetra-antennary complex N-glycans are

495   also observed which can be fully sialylated (for example peaks at m/z 3776

496   and 4587). Therefore, the glycomic analysis revealed that both Asn-221 and

497   Asn-575 contained larger, more highly processed N-glycans that are not

498   observed on the IgG1-Fc control (Fig. 9 and supplemental Figs. S2-S4). As

499   predicted, no glycans could be detected on the glycosylation-deficient double

500   mutants (N297A/N563A/C575A and C309L/N297A/N563A/C575A).

501

502

503   ***The Asn^{221} glycan imparts enhanced binding to influenza hemagglutinin***

504   To determine if any of the hyper-sialylated Fc mutants possessed biologically

505   useful properties, we investigated their binding to hemagglutinin, a prototypic

506   viral sialic-acid binding ligand (Fig. 10A, 10B). We used clinically available

507   IVIG as a positive control, as IVIG is known to contain high concentrations of

508   IgG antibodies against a diverse range of influenza hemagglutinins (38).

509   As expected, IVIG bound strongly to recombinant hemagglutinin from

510   both influenza A and B viruses (Fig. 10A, 10B). With the exception of the

511   aglycosylated mutants (C309L/N297A/N563A/C575A and

512   N297A/N563A/C575A) and the IgG1-Fc control, all the glycan-modified Fc

513   fragments bound recombinant hemagglutinin from both group A and B

514   viruses. Binding was also reflected in the abundance of sialylated N-glycans

515   of the mutant proteins (supplemental Figs. S2-S4). Thus, mutants containing

516   Asn^{221} bound more strongly than their equivalents in which Asn^{221} was absent

517   (Fig. 10A, 10B).

518   Although binding to native inactivated influenza strain A New

519 Caledonia/20/99 virus (H1N1) was poorer than binding to either recombinant

520 hemagglutinins from influenza A (Shantou) or influenza B (Florida)

521 respectively, two mutants (D221N/C309L/N297A/C575A and D221N/C575A)

522 showed superior binding to the native virus compared to either IVIG or their

523 equivalent mutants in which Asn[221] was absent (compare C575A with

524 D221N/C575A) (Fig. 10A, 10B).

525

526 ***Asn[221]-containing mutants inhibit hemagglutination by influenza***

527 To test if the binding to hemagglutinin has any functional relevance, we used

528 the World Health Organization (WHO)-based hemagglutination inhibition (HI)

529 protocol to quantify influenza-specific inhibitory titers of the mutants that

530 bound the native virus strongly (Fig. 10C). Both D221N/C309L/N297A/C575A

531 and D221N/C575A prevented hemagglutination by New Caledonia/20/99 virus

532 (H1N1) at concentrations as low as $0.1\mu M$ and were demonstrably more

533 effective than molar equivalents of either IVIG or anti-H1N1 polyclonal IgG.

534   In contrast, the equivalent molecules that lack Asn[221], i.e.

535 C309L/N297A/C575A and C575A, failed to inhibit hemagglutination although

536 partial inhibition was observed with the C575A mutant at the highest

537 concentrations in some experiments (Fig. 10C). Hence, receptor binding of

538 influenza A viruses is competed out only by mutants in which Asn[221] and

539 Asn[563] are present. That both mutants run entirely as monomers by SEC-

540 HPLC (supplemental Fig. S1C) shows that the disposition of the glycans at

541 the N- and C-terminii of the Fc are more favorably orientated for binding

542 native viral hemagglutinin in monomers than multimers.

543

544

545

546

547

548

549

550

Discussion

Many groups have postulated that multivalent Fc constructs have potential for the treatment of immune conditions involving pathogenic antibodies (2, 5, 39, 40), and a recent study has shown that hexavalent Fcs can block FcγRs leading to their down-modulation and prolonged disruption of FcγR effector functions both *in vitro* and *in vivo* (41, 42). Hexameric Fcs have also been shown to inhibit platelet phagocytosis in mouse models of ITP (41, 43).

Although disulfide bonded hexameric Fcs may provide exciting new treatment approaches to control autoimmune diseases, they are more difficult to manufacture than smaller simpler Fc molecules. Their beneficial effects must also be carefully balanced with the acute risk of pro-inflammatory responses observed upon FcγR cross-linking, and the increased risk from infection or cancers due to long-term immune suppression. These potential drawbacks with multimeric Fcs led us to investigate if complex monomers may be developed that retain the advantages of multimers, e.g. high-avidity binding to low-affinity receptors, but that are also more readily manufactured to scale.

Although Fc engineering by mutagenesis and/or direct modification to the Asn[297] glycan have yielded modified affinity and/or selectivity for FcγRs (1, 18, 44–49), interactions with glycan receptors have largely been ignored despite a large body of literature demonstrating their importance in controlling unwanted inflammation (50–53). However, such approaches that show enhanced receptor interactions via mutations introduced into full-length IgG molecules (54–56) may not necessarily be predictive *a priori* in the context of either Fc multimers or their Fc fragments (24, 41).

Furthermore, reported Fc mutations or glycan modifications have mostly focused on the conserved Asn[297] glycan that is largely buried within the Fc (4, 17–20), and thus monomeric IgG1 is unable to interact with a broad range of glycan receptors (Fig. 11A). Although Siglec-2 (36), DC-SIGN (2, 57, 58), DCIR (35), and FcRL5 (2, 59) have all recently been shown to be ligands for IVIG, these interactions may also stem from specific Fab-mediated binding (60). Thus, glycosylation of intact IgG is known to be critically important, but the relative contribution of the Fc, Fab, and/or their attached glycans, together

17

584   with the identity of the salient receptors involved in IVIG efficacy, remain

585   controversial.

586   We took an alternative approach to glycan modification by introducing,

587   in various combinations, two additional N-linked glycosylation sites (Asn^{221}

588   and Asn^{563}) into our hexa-Fc (2, 24). To investigate the effects of this

589   additional glycosylation, hexa-Fc was further mutated to remove one (Fig. 1)

590   or both of the cysteine residues (Cys^{309} and Cys^{575}) (Fig. 2) that are required

591   for inter-disulfide bond formation between individual Fc moieties in hexa-Fc.

592   This approach yielded complex glycosylated molecules (Fig. 3, Fig. 9 and

593   Supplemental Figs. S2-S4), including the monomeric D221N/C309L/C575A

594   mutant that has all three glycans attached, and which showed improved

595   binding to FcγRIIB, DC-SIGN, and DCIR; these receptors being implicated in

596   the efficacy of IVIG (Table 1) (8, 17, 20, 61, 62). The tri-glycan mutant

597   (D221N/C309L/C575A) also bound more strongly and broadly to all the glycan

598   receptors investigated, including receptors recently implicated in IVIG efficacy

599   e.g., CD23 (63), CD22 (36), and DCIR (clec4a) (35), when compared to

600   mono-glycosylated (e.g. IgG1-Fc) or non-glycosylated

601   (C309L/N297A/N563A/C575A) controls (Fig. 4, Table 1).

602   The observed binding to CD22 was particularly surprising as this

603   receptor prefers α-2,6 linked neuraminic acid and not α-2,3 linkages attached

604   by CHO-K1 cells, although proximity labeling experiments have recently

605   shown that glycan-independent interactions of CD22/Siglec-2 with

606   immunoglobulin in the B-cell receptor is possible (64).

607   We also observed marked binding of D221N/C309L/C575A to dectins

608   (Fig. 4), receptors that more typically recognize β-1,3-glucans expressed by

609   fungal pathogens (65). Although dectin-1 is known to bind variably

610   glycosylated human tetraspanins CD37 and CD63 (66), the anti-inflammatory

611   activity of IgG1 immune complexes may be mediated by Fc galactosylation

612   and associations with dectin-1 and FcγRIIB (67).

613   The insertion of multiple glycan sites into the Fc, in particular at Asn^{221},

614   enables new receptor interactions that are not possible with solely Asn^{297}-

615   directed approaches (Fig. 11A). For example, we generated the di-glycan

616   D221N/C309L/N297A/C575A mutant that displayed marked binding to Siglec-

617 1 and Siglec-4 (MAG), both receptors being clinically implicated in the control

618 of neuropathy (25, 26). This mutant showed no observable binding to either

619 FcγRs or complement proteins (Tables 2, 3) yet was highly effective at

620 blocking hemagglutination by influenza A virus (Fig. 10C).

621   As glycan-mediated binding is essential for the influenza virus to infect

622 cells of the respiratory tract, mutations in hemagglutinin that lead to loss of

623 receptor binding are unlikely to survive any neutralizing antibodies induced

624 during an immune response (Fig. 11B). Modelling of the D221N/C575A

625 mutant shows that the distance from the N-terminal to the C-terminal tips of

626 the Fc is ~60Å (Fig. 11B), which is the same distance between the sialic-acid

627 binding domains on the hemagglutinin trimer (68). The Asn[221] and Asn[563]

628 sugars located at the tips of the Fc are not constrained by their location within

629 the Fc, as with Asn[297], and would therefore be expected to be highly mobile

630 and flexible with respect of searching out the hemagglutinin binding pocket.

631   Alternative anti-influenza therapeutic strategies are urgently needed.

632 The use of IVIG during the 2009 and 1918 pandemics reduced mortality from

633 influenza by 26% and 50% respectively (69, 70), and a recent randomized,

634 placebo-controlled study suggests these figures may be improved by

635 enhancing influenza-specific antibodies in IVIG (Flu-IVIG) preparations (38).

636 As Flu-IVIG is manufactured in advance of future epidemics, there may be

637 modest or no neutralizing activity against emerging strains. Combinations of

638 Flu-IVIG or neuraminidase inhibitor drugs with Fc sialic-acid binding domain

639 blockers may enhance the efficacy of Flu-IVIG or neuraminidase inhibitor-

640 based medicines. Neither the D221N/C575A nor

641 D221N/C309L/N297A/C575A mutants that inhibited hemagglutination so

642 effectively (Fig. 10C), bind FcγRIIIA (Fig. 6 and Table 2), and would thus not

643 be expected to interfere with FcγRIIIA dependent ADCC toward influenza-

644 infected cells by neutralizing IgG present in Flu-IVIG.

645   As well as direct hemagglutinin binding, the molecules may shield sialic

646 acid receptor binding sites on epithelial cells, or act as decoy receptors

647 through receptor mimicry thereby preventing binding of the virus to epithelial

648 target cells. Similarly, being rich in sialic acid the molecules may also act as

649 decoy substrates for neuraminidase. Intranasal delivery of Fc fragments may

650   therefore be feasible, as Fc-fused interleukin-7 can provide long-lasting

651   prophylaxis against lethal influenza virus after intranasal delivery (71). We

652   have previously shown that Fc multimers can bind the neonatal Fc-receptor

653   (FcRn) (72). Thus binding to the neonatal FcRn may act to increase the

654   residence time of Fc blockers delivered to the lung (73, 74).

655   A potential drawback to the hyper-sialylation approach with respect to

656   blocking hemagglutinin may be the susceptibility of Fc glycans to viral

657   neuraminidase. Although neuraminidase from *Clostridium perfringens* could

658   catalyze the hydrolysis of sialic acid residues from our soluble Fc fragments

659   and thus block interactions with glycan receptors (supplementary Fig. S1B), it

660   remains to be tested if hemagglutinin-bound Fcs are susceptible to catalysis

661   by the influenza neuraminidase. We believe that metabolic oligosaccharide

662   engineering with alkyne sialic acids could create neuraminidase-resistant Fc

663   blockers (75).

664   In another example, multiple mutants were shown to bind DEC-205

665   (Figs. 4, 5, Table 1), the major endocytic receptor expressed by dendritic

666   cells, which suggests that these constructs may be useful for the targeted

667   delivery of antigens in vaccines. Current approaches to deliver antigen to

668   DEC-205 rely on DEC-205-specific delivery, often with antigens fused to anti-

669   DEC-205 mAbs (76–78), whereas approaches that target multiple DC

670   receptors, including DEC-205, may make for more effective antigen delivery.

671   To be useful in vaccines, an antigen must cluster through the binding of

672   multiple Fc regions in near-neighbor interactions with multiple low-affinity

673   FcγRs (79), and in particular FcγRIIA, FcγRIIB and FcγRIIIA (79–81). As

674   described above we generated multimers with differential binding to either

675   FcγRIIB (e.g. N297A/N563A/C575A), FcγRIIIA (e.g. C309L and

676   D221N/N563A/C575A) or with a capability to bind both FcγRIIB and FcγRIIIA

677   (e.g. N563A/C575A). Multimers formed by the N563A/C575A or

678   C309L/N563A/C575A mutants may be particularly relevant, as these were

679   also able to bind type 2 glycan receptors and activate the complement

680   cascade, both implicated in the efficacy of vaccines (5).

681   We also created molecules disrupted for covalent bonding (the double

682   cysteine knockouts) that formed multimers in solution through non-covalent

683   tailpiece clustering (e.g. C309L/N563A/C575A and

684   D221N/C309L/N563A/C575A) that showed enhanced interactions with FcγRs,

685   in particular FcγRIIIA (Figs. 6 and 7). Whether these will be more effective

686   than covalently stabilized Fcs (e.g. N563A/C575A) at enhancing FcγRIIIA-

687   mediated effector functions, in for example therapeutic mAbs or Fc-fusion

688   therapies/vaccines, remains to be determined.

689   As summarized in Tables 1-3, we identified: *i*) mutant Fc molecules that

690   are capable of binding C1q and activating complement, but that show little or

691   no detectable interaction with either FcγRs or glycan receptors; *ii*) molecules

692   with enhanced activation of complement, improved binding to FcγRs and little

693   engagement of glycan receptors; *iii*) molecules with enhanced binding to C1q

694   but little C5b-9 deposition that retain interaction with both Fcγ and glycan

695   receptors, and *iv*) monomeric molecules with enhanced binding to a subset of

696   sialic-acid-dependent glycan receptors, in particular Siglec-1, Siglec-4 and

697   hemagglutinin, with little or no interaction with either FcγRs or complement.

698   Consequently, by adding or removing glycosylation and/or disulfide-

699   bonding sites within our original hexameric Fc platform (2, 5, 24), new

700   repertoires of desirable binding attributes can be made. These molecules may

701   be useful in the control of other pathogens, including Newcastle Disease

702   Virus, group B streptococci, *Streptococcus pneumoniae*, and *Mycoplasma*

703   *genitalium*, in which sialic-acid dependent interactions are also crucially

704   important (82).

705

715

Author contributions

716 **Author contributions**

717 R.J.P. conceived and designed the overall study. R.J.P, P.A.B. and D.L.

718 designed and performed experiments. M.W. ran our SEC-HPLC samples.

719 R.J.P. wrote the manuscript, and all authors commented on drafts and

720 reviewed the final manuscript.

721

722

723

724

725

726

727

728

729

730

731

732

733

734

735

736

737

738

739

740

741

742

743

744

745

746 **References**

747

748 1. Dalziel, M., M. Crispin, C. N. Scanlan, N. Zitzmann, and R. A. Dwek. 2014.

749 Emerging principles for the therapeutic exploitation of glycosylation. *Science*

750   343: 1235681–1235687.

751   2. Czajkowsky, D. M., J. T. Andersen, A. Fuchs, T. J. Wilson, D. Mekhaiel, M.

752   Colonna, J. He, Z. Shao, D. a. Mitchell, G. Wu, A. Dell, S. Haslam, K. a.

753   Lloyd, S. C. Moore, I. Sandlie, P. a. Blundell, and R. J. Pleass. 2015.

754   Developing the IVIG biomimetic, Hexa-Fc, for drug and vaccine applications.

755   *Sci. Rep.* 5: 9526.

756   3. Shields, R. L., J. Lai, R. Keck, L. Y. O'Connell, K. Hong, Y. Gloria Meng, S.

757   H. A. Weikert, and L. G. Presta. 2002. Lack of fucose on human IgG1 N-

758   linked oligosaccharide improves binding to human FcγRIII and antibody-

759   dependent cellular toxicity. *J. Biol. Chem.* 277: 26733–26740.

760   4. Lux, A., X. Yu, C. N. Scanlan, and F. Nimmerjahn. 2013. Impact of Immune

761   Complex Size and Glycosylation on IgG Binding to Human FcγRs. *J.*

762   *Immunol.* 190: 4315–4323.

763   5. Czajkowsky, D. M., J. Hu, Z. Shao, and R. J. Pleass. 2012. Fc-fusion

764   proteins: New developments and future perspectives. *EMBO Mol. Med.* 4:

765   1015–1028.

766   6. Debre, M., M. C. Bonnet, W. H. Fridman, E. Carosella, N. Philippe, P.

767   Reinert, E. Vilmer, C. Kaplan, J. L. Teillaud, and C. Griscelli. 1993. Infusion of

768   Fc gamma fragments for treatment of children with acute immune

769   thrombocytopenic purpura. *Lancet* 342: 945–949.

770   7. Anthony, R. M., F. Nimmerjahn, D. J. Ashline, V. N. Reinhold, J. C.

771   Paulson, and J. V Ravetch. 2008. Recapitulation of IVIG Anti-Inflammatory

772   Activity with a Recombinant IgG Fc. *Science* 320: 373–376.

773   8. Anthony, R. M., T. Kobayashi, F. Wermeling, and J. V. Ravetch. 2011.

774   Intravenous gammaglobulin suppresses inflammation through a novel T(H)2

775   pathway: Commentary. *Nature* 475: 110–113.

776   9. Liu, L. 2015. Antibody glycosylation and its impact on the pharmacokinetics

777   and pharmacodynamics of monoclonal antibodies and Fc-fusion proteins. *J.*

778   *Pharm. Sci.* 104: 1866–1884.

779   10. Li, H., N. Sethuraman, T. A. Stadheim, D. Zha, B. Prinz, N. Ballew, P.

780   Bobrowicz, B.-K. Choi, W. J. Cook, M. Cukan, N. R. Houston-Cummings, R.

781   Davidson, B. Gong, S. R. Hamilton, J. P. Hoopes, Y. Jiang, N. Kim, R.

782   Mansfield, J. H. Nett, S. Rios, R. Strawbridge, S. Wildt, and T. U. Gerngross.

783   2006. Optimization of humanized IgGs in glycoengineered Pichia pastoris.

784 *Nat. Biotechnol.* 24: 210–5.

785 11. Pepinsky, R. B., Z. Shao, B. Ji, Q. Wang, G. Meng, L. Walus, X. Lee, Y.

786 Hu, C. Graff, E. Garber, W. Meier, and S. Mi. 2011. Exposure levels of anti-

787 LINGO-1 Li81 antibody in the central nervous system and dose-efficacy

788 relationships in rat spinal cord remyelination models after systemic

789 administration. *J. Pharmacol. Exp. Ther.* 339: 519–29.

790 12. St-Amour, I., I. Paré, W. Alata, K. Coulombe, C. Ringuette-Goulet, J.

791 Drouin-Ouellet, M. Vandal, D. Soulet, R. Bazin, and F. Calon. 2013. Brain

792 bioavailability of human intravenous immunoglobulin and its transport through

793 the murine blood-brain barrier. *J. Cereb. Blood Flow Metab.* 33: 1983–1992.

794 13. Hawkins, C. P., P. M. G. Munro, F. Mackenzie, J. Kesselring, P. S. Tofts,

795 E. P. G. H. Du Boulay, D. N. Landon, and W. I. Mcdonald. 1990. Duration and

796 selectivity of blood-brain barrier breakdown in chronic relapsing experimental

797 allergic encephalomyelitis studied by gadolinium-dtpa and protein markers.

798 *Brain* 113: 365–378.

799 14. Xu, J., L. Zhao, Y. Zhang, Q. Guo, and H. Chen. 2016. CD16 and CD32

800 Gene Polymorphisms May Contribute to Risk of Idiopathic Thrombocytopenic

801 Purpura. *Med. Sci. Monit.* 22: 2086–2096.

802 15. Zhang, G., C. A. Massaad, T. Gao, L. Pillai, N. Bogdanova, S. Ghauri, and

803 K. A. Sheikh. 2016. Sialylated intravenous immunoglobulin suppress anti-

804 ganglioside antibody mediated nerve injury. *Exp. Neurol.* 282: 49–55.

805 16. Finke, J. M., K. R. Ayres, R. P. Brisbin, H. A. Hill, E. E. Wing, and W. A.

806 Banks. 2017. Antibody blood-brain barrier efflux is modulated by glycan

807 modification. *Biochim. Biophys. Acta - Gen. Subj.* 1861: 2228–2239.

808 17. Washburn, N., I. Schwab, D. Ortiz, N. Bhatnagar, J. C. Lansing, A.

809 Medeiros, S. Tyler, D. Mekala, E. Cochran, H. Sarvaiya, K. Garofalo, R.

810 Meccariello, J. W. Meador, L. Rutitzky, B. C. Schultes, L. Ling, W. Avery, F.

811 Nimmerjahn, A. M. Manning, G. V. Kaundinya, and C. J. Bosques. 2015.

812 Controlled tetra-Fc sialylation of IVIg results in a drug candidate with

813 consistent enhanced anti-inflammatory activity. *Proc. Natl. Acad. Sci. U. S. A.*

814 112: 201422481.

815 18. Yu, X., K. Baruah, D. J. Harvey, S. Vasiljevic, D. S. Alonzi, B. D. Song, M.

816 K. Higgins, T. A. Bowden, C. N. Scanlan, and M. Crispin. 2013. Engineering

817 hydrophobic protein-carbohydrate interactions to fine-tune monoclonal

818   antibodies. *J. Am. Chem. Soc.* 135: 9723–9732.

819   19. Dekkers, G., R. Plomp, C. A. M. Koeleman, R. Visser, H. H. von Horsten,

820   V. Sandig, T. Rispens, M. Wuhrer, and G. Vidarsson. 2016. Multi-level glyco-

821   engineering techniques to generate IgG with defined Fc-glycans. *Sci. Rep.* 6:

822   36964.

823   20. Pagan, J. D., M. Kitaoka, and R. M. Anthony. 2017. Engineered Sialylation

824   of Pathogenic Antibodies In Vivo Attenuates Autoimmune Disease. *Cell* 172:

825   1–14.

826   21. Baldo, B. A. 2015. Chimeric Fusion Proteins Used for Therapy:

827   Indications, Mechanisms, and Safety. *Drug Saf.* 38: 455–479.

828   22. Boesch, A. W., E. P. Brown, H. D. Cheng, M. O. Ofori, E. Normandin, P.

829   A. Nigrovic, G. Alter, and M. E. Ackerman. 2014. Highly parallel

830   characterization of IgG Fc binding interactions. *MAbs* 6: 915–927.

831   23. Crispin, M., X. Yu, and T. a. Bowden. 2013. Crystal structure of sialylated

832   IgG Fc: Implications for the mechanism of intravenous immunoglobulin

833   therapy. *Proc. Natl. Acad. Sci.* 110: 3544–3546.

834   24. Blundell, P. A., N. P. L. Le, J. Allen, Y. Watanabe, and R. J. Pleass. 2017.

835   Engineering the fragment crystallizable (Fc) region of human IgG1 multimers

836   and monomers to fine-tune interactions with sialic acid-dependent receptors.

837   *J. Biol. Chem.* 292: 12994–13007.

838   25. Zhang, G., C. A. Massaad, T. Gao, L. Pillai, N. Bogdanova, S. Ghauri, and

839   K. A. Sheikh. 2016. Sialylated intravenous immunoglobulin suppress anti-

840   ganglioside antibody mediated nerve injury. *Exp. Neurol.* 282: 49–55.

841   26. Wong, A. H. Y., Y. Fukami, M. Sudo, N. Kokubun, S. Hamada, and N.

842   Yuki. 2016. Sialylated IgG-Fc: a novel biomarker of chronic inflammatory

843   demyelinating polyneuropathy. *J. Neurol. Neurosurg. Psychiatry* 87: 275–9.

844   27. Thomas, R. J. 2010. Receptor mimicry as novel therapeutic treatment for

845   biothreat agents. *Bioeng. Bugs* 1: 17–30.

846   28. Subedi, G. P., Q. M. Hanson, and A. W. Barb. 2014. Restricted Motion of

847   the Conserved Immunoglobulin G1 N-Glycan Is Essential for Efficient FcγRIIIa

848   Binding. *Structure* 22: 1478–1488.

849   29. Frank, M., R. C. Walker, W. N. Lanzilotta, J. H. Prestegard, and A. W.

850   Barb. 2014. Immunoglobulin G1 Fc domain motions: Implications for Fc

851   engineering. *J. Mol. Biol.* 426: 1799–1811.

852   30. Pincetic, A., S. Bournazos, D. J. DiLillo, J. Maamary, T. T. Wang, R.

853   Dahan, B.-M. Fiebiger, and J. V Ravetch. 2014. Type I and type II Fc

854   receptors regulate innate and adaptive immunity. *Nat. Immunol.* 15: 707–716.

855   31. Mekhaiel, D. N. A., D. M. Czajkowsky, J. T. Andersen, J. Shi, M. El-

856   Faham, M. Doenhoff, R. S. McIntosh, I. Sandlie, J. He, J. Hu, Z. Shao, and R.

857   J. Pleass. 2011. Polymeric human Fc-fusion proteins with modified effector

858   functions. *Sci. Rep.* 1: 124.

859   32. North, S. J., J. Jang-Lee, R. Harrison, K. Canis, M. N. Ismail, A. Trollope,

860   A. Antonopoulos, P. C. Pang, P. Grassi, S. Al-Chalabi, A. T. Etienne, A. Dell,

861   and S. M. Haslam. 2010. Mass spectrometric analysis of mutant mice.

862   *Methods Enzymol.* 478: 27–77.

863   33. Ceroni, A., K. Maass, H. Geyer, R. Geyer, A. Dell, and S. M. Haslam.

864   2008. GlycoWorkbench: A tool for the computer-assisted annotation of mass

865   spectra of glycans. *J. Proteome Res.* 7: 1650–1659.

866   34. Spirig, R., I. K. Campbell, S. Koernig, C.-G. Chen, B. J. B. Lewis, R.

867   Butcher, I. Muir, S. Taylor, J. Chia, D. Leong, J. Simmonds, P. Scotney, P.

868   Schmidt, L. Fabri, A. Hofmann, M. Jordi, M. O. Spycher, S. Cattepoel, J.

869   Brasseit, C. Panousis, T. Rowe, D. R. Branch, A. Baz Morelli, F. Käsermann,

870   and A. W. Zuercher. 2018. rIgG1 Fc Hexamer Inhibits Antibody-Mediated

871   Autoimmune Disease via Effects on Complement and FcγRs. *J. Immunol.*

872   200: 2542–2553.

873   35. Massoud, A. H., M. Yona, D. Xue, F. Chouiali, H. Alturaihi, A. Ablona, W.

874   Mourad, C. A. Piccirillo, and B. D. Mazer. 2014. Dendritic cell

875   immunoreceptor: A novel receptor for intravenous immunoglobulin mediates

876   induction of regulatory T cells. *J. Allergy Clin. Immunol.* 133: 853–863.

877   36. Seite, J. F., D. Cornec, Y. Renaudineau, P. Youinou, R. A. Mageed, and

878   S. Hillion. 2010. IVIg modulates BCR-signaling through CD22 and promotes

879   apoptosis in mature human B lymphocytes. *Blood* 116: 1686–1704.

880   37. Czajkowsky, D. M., J. T. Andersen, A. Fuchs, T. J. Wilson, D. Mekhaiel,

881   M. Colonna, J. He, Z. Shao, D. A. Mitchell, G. Wu, A. Dell, S. Haslam, K. A.

882   Lloyd, S. C. Moore, I. Sandlie, P. A. Blundell, and R. J. Pleass. 2015.

883   Developing the IVIG biomimetic, Hexa-Fc, for drug and vaccine applications.

884   *Sci. Rep.* 5: 9526.

885   38. Vanderven, H. A., K. Wragg, F. Ana-Sosa-Batiz, A. B. Kristensen, S.

886   Jegaskanda, A. K. Wheatley, D. Wentworth, B. D. Wines, P. M. Hogarth, S.

887   Rockman, and S. J. Kent. 2018. Anti-influenza Hyperimmune Immunoglobulin

888   Enhances Fc-functional Antibody Immunity during Human Influenza Infection.

889   *J. Infect. Dis.* 218: 1383-1393.

890   39. Jain, A., H. S. Olsen, R. Vyzasatya, E. Burch, Y. Sakoda, E. Y. Mérigeon,

891   L. Cai, C. Lu, M. Tan, K. Tamada, D. Schulze, D. S. Block, and S. E. Strome.

892   2012. Fully recombinant IgG2a Fc multimers (stradomers) effectively treat

893   collagen-induced arthritis and prevent idiopathic thrombocytopenic purpura in

894   mice. *Arthritis Res. Ther.* 14: R192: 1-12.

895   40. Ortiz, D. F., J. C. Lansing, L. Rutitzky, E. Kurtagic, T. Prod, A. Choudhury,

896   N. Washburn, N. Bhatnagar, C. Beneduce, K. Holte, R. Prenovitz, M. Child, J.

897   Killough, S. Tyler, J. Brown, S. Nguyen, I. Schwab, M. Hains, R. Meccariello,

898   L. Markowitz, J. Wang, R. Zouaoui, A. Simpson, B. Schultes, I. Capila, L.

899   Ling, F. Nimmerjahn, A. M. Manning, and C. J. Bosques. 2016. Elucidating

900   the interplay between IgG-Fc valency and Fc g R activation for the design of

901   immune complex inhibitors. *Sci Transl Med* 8: 365–370.

902   41. Qureshi, O. S., T. F. Rowley, F. Junker, S. J. Peters, S. Crilly, J.

903   Compson, A. Eddleston, H. Björkelund, K. Greenslade, M. Parkinson, N. L.

904   Davies, R. Griffin, T. L. Pither, K. Cain, L. Christodoulou, L. Staelens, E.

905   Ward, J. Tibbitts, A. Kiessling, B. Smith, F. R. Brennan, M. Malmqvist, F.

906   Fallah-Arani, and D. P. Humphreys. 2017. Multivalent Fcγ-receptor

907   engagement by a hexameric Fc-fusion protein triggers Fcγ-receptor

908   internalisation and modulation of Fcγ-receptor functions. *Sci. Rep.* 7: 17049.

909   42. Rowley, T. F., S. J. Peters, M. Aylott, R. Griffin, N. L. Davies, L. J. Healy,

910   R. M. Cutler, A. Eddleston, T. L. Pither, J. M. Sopp, O. Zaccheo, G. Fossati,

911   K. Cain, A. M. Ventom, H. Hailu, E. J. Ward, J. Sherington, F. R. Brennan, F.

912   Fallah-Arani, and D. P. Humphreys. 2018. Engineered hexavalent Fc proteins

913   with enhanced Fc-gamma receptor avidity provide insights into immune-

914   complex interactions. *Commun. Biol.* 1: 146.

915   43. Lewis, BJ., Spirig, R., Kasermann, F., Branch, D. 2017. No Title. In *27th*

916   *Regional Congress of the International Society of Blood Transfusion* Embase

917   Vox Sanguinis, Copenhagen. 21.

918   44. Lund, J., J. D. Pound, P. T. Jones, A. R. Duncan, T. Bentley, M. Goodall,

919   B. A. Levine, R. Jefferis, and G. Winte. 1992. Multiple binding sites on the

920 CH2 domain of IgG for mouse FcγRII. *Mol. Immunol.* 29: 53–59.

921 45. Lund, J., N. Takahashi, J. D. Pound, M. Goodall, and R. Jefferis. 1996.

922 Multiple Interactions of IgG with Its Core Oligosaccharide Can Modulate

923 Recognition by Complement and Human Fcγ Receptor I and Influence the

924 Synthesis of Its Oligosaccharide Chains. *J. Immunol.* 157: 4963–4969.

925 46. Jefferis, R., J. Lund, and J. D. Pound. 1998. IgG-Fc-mediated effector

926 functions: Molecular definition of interaction sites for effector ligands and the

927 role of glycosylation. *Immunol. Rev.* 163: 59–76.

928 47. Houde, D., Y. Peng, S. A. Berkowitz, and J. R. Engen. 2010. Post-

929 translational modifications differentially affect IgG1 conformation and receptor

930 binding. *Mol Cell Proteomics* 9: 1716–1728.

931 48. Woof, J. M., and D. R. Burton. 2004. Human antibody-Fc receptor

932 interactions illuminated by crystal structures. *Nat. Rev. Immunol.* 4: 89–99.

933 49. Saxena, A., and D. Wu. 2016. Advances in therapeutic Fc engineering -

934 modulation of IgG-associated effector functions and serum half-life. *Front.*

935 *Immunol.* 8: 38–53.

936 50. MacAuley, M. S., P. R. Crocker, and J. C. Paulson. 2014. Siglec-mediated

937 regulation of immune cell function in disease. *Nat. Rev. Immunol.* 14: 653–

938 666.

939 51. Bochner, B. S., and N. Zimmermann. 2015. Role of siglecs and related

940 glycan-binding proteins in immune responses and immunoregulation. *J.*

941 *Allergy Clin. Immunol.* 135: 598–608.

942 52. Mahajan, V. S., and S. Pillai. 2016. Sialic acids and autoimmune disease.

943 *Immunol. Rev.* 269: 145–161.

944 53. Büll, C., T. Heise, G. J. Adema, and T. J. Boltje. 2016. Sialic Acid

945 Mimetics to Target the Sialic Acid-Siglec Axis. *Trends Biochem. Sci.* 41: 519–

946 531.

947 54. Shields, R. L., J. Lai, R. Keck, L. Y. O'Connell, K. Hong, Y. G. Meng, S. H.

948 A. Weikert, and L. G. Presta. 2002. Lack of Fucose on Human IgG1 N-Linked

949 Oligosaccharide Improves Binding to Human FcγRIII and Antibody-

950 dependent Cellular Toxicity . *J. Biol. Chem.* 277: 26733–26740.

951 55. Shields, R. L., A. K. Namenuk, K. Hong, Y. G. Meng, J. Rae, J. Briggs, D.

952 Xie, J. Lai, A. Stadlen, B. Li, J. A. Fox, and L. G. Presta. 2001. High

953 Resolution Mapping of the Binding Site on Human IgG1 for FcγRI, FcγRII,

954 FcγRIII, and FcRn and Design of IgG1 Variants with Improved Binding to the

955 FcγR. *J. Biol. Chem.* 276: 6591–6604.

956 56. Moore, G. L., H. Chen, S. Karki, and G. A. Lazar. 2010. Engineered Fc

957 variant antibodies with enhanced ability to recruit complement and mediate

958 effector functions. *MAbs* 2: 181–189.

959 57. Fiebiger, B. M., J. Maamary, A. Pincetic, and J. V. Ravetch. 2015.

960 Protection in antibody- and T cell-mediated autoimmune diseases by

961 antiinflammatory IgG Fcs requires type II FcRs. *Proc. Natl. Acad. Sci.* 112:

962 2385–2394.

963 58. Schwab, I., M. Biburger, G. Krönke, G. Schett, and F. Nimmerjahn. 2012.

964 IVIg-mediated amelioration of ITP in mice is dependent on sialic acid and

965 SIGNR1. *Eur. J. Immunol.* 42: 826–830.

966 59. Franco, A., B. Damdinsuren, T. Ise, J. Dement-Brown, H. Li, S. Nagata,

967 and M. Tolnay. 2013. Human Fc Receptor-Like 5 Binds Intact IgG via

968 Mechanisms Distinct from Those of Fc Receptors. *J. Immunol.* 190: 5739–

969 5746.

970 60. van de Bovenkamp, F. S., L. Hafkenscheid, T. Rispens, and Y. Rombouts.

971 2016. The Emerging Importance of IgG Fab Glycosylation in Immunity. *J.*

972 *Immunol.* 196: 1435–41.

973 61. Kaneko, Y., F. Nimmerjahn, and J. V Ravetch. 2006. Anti-inflammatory

974 activity of immunoglobulin G resulting from Fc sialylation. *Science* 313: 670–3.

975 62. Tackenberg, B., I. Jelcic, A. Baerenwaldt, W. H. Oertel, N. Sommer, F.

976 Nimmerjahn, and J. D. Lünemann. 2009. Impaired inhibitory Fcgamma

977 receptor IIB expression on B cells in chronic inflammatory demyelinating

978 polyneuropathy. *Proc. Natl. Acad. Sci. U. S. A.* 106: 4788–92.

979 63. Wang, T. T., J. Maamary, G. S. Tan, S. Bournazos, C. W. Davis, F.

980 Krammer, S. J. Schlesinger, P. Palese, R. Ahmed, and J. V. Ravetch. 2015.

981 Anti-HA Glycoforms Drive B Cell Affinity Selection and Determine Influenza

982 Vaccine Efficacy. *Cell* 162: 160–169.

983 64. Alborzian Deh Sheikh, A., C. Akatsu, A. Imamura, H. H. M. Abdu-Allah, H.

984 Takematsu, H. Ando, H. Ishida, and T. Tsubata. 2018. Proximity labeling of

985 cis-ligands of CD22/Siglec-2 reveals stepwise α2,6 sialic acid-dependent and

986 -independent interactions. *Biochem. Biophys. Res. Commun.* 495: 854–859.

987 65. Geijtenbeek, T. B. H., and S. I. Gringhuis. 2009. Signalling through C-type

988 lectin receptors: Shaping immune responses. *Nat. Rev. Immunol.* 9: 465–479.

989 66. Meyer-Wentrup, F., C. G. Figdor, M. Ansems, P. Brossart, M. D. Wright,

990 G. J. Adema, and A. B. van Spriel. 2007. Dectin-1 Interaction with Tetraspanin

991 CD37 Inhibits IL-6 Production. *J. Immunol.* 178: 154–162.

992 67. Karsten, C. M., M. K. Pandey, J. Figge, R. Kilchenstein, P. R. Taylor, M.

993 Rosas, J. U. McDonald, S. J. Orr, M. Berger, D. Petzold, V. Blanchard, A.

994 Winkler, C. Hess, D. M. Reid, I. V Majoul, R. T. Strait, N. L. Harris, G. Köhl, E.

995 Wex, R. Ludwig, D. Zillikens, F. Nimmerjahn, F. D. Finkelman, G. D. Brown,

996 M. Ehlers, and J. Köhl. 2012. Anti-inflammatory activity of IgG1 mediated by

997 Fc galactosylation and association of FcγRIIB and dectin-1. *Nat. Med.* 18:

998 1401–6.

999 68. Xu, R., D. C. Ekiert, J. C. Krause, R. Hai, J. E. Crowe, and I. A. Wilson.

1000 2010. Structural basis of preexisting immunity to the 2009 H1N1 pandemic

1001 influenza virus. *Science* 328: 357–360.

1002 69. Hung, I. F. N., K. K. W. To, C.-K. Lee, K.-L. Lee, W.-W. Yan, K. Chan, W.-

1003 M. Chan, C.-W. Ngai, K.-I. Law, F.-L. Chow, R. Liu, K.-Y. Lai, C. C. Y. Lau, S.-

1004 H. Liu, K.-H. Chan, C.-K. Lin, and K.-Y. Yuen. 2013. Hyperimmune IV

1005 immunoglobulin treatment: a multicenter double-blind randomized controlled

1006 trial for patients with severe 2009 influenza A(H1N1) infection. *Chest* 144:

1007 464–473.

1008 70. Luke, T. C., E. M. Kilbane, J. L. Jackson, and S. L. Hoffman. 2006. Meta-

1009 analysis: Convalescent blood products for Spanish influenza pneumonia: A

1010 future H5N1 treatment? *Ann. Intern. Med.* 145: 599–609.

1011 71. Kang, M. C., D.-H. Choi, Y. W. Choi, S. J. Park, H. Namkoong, K. S. Park,

1012 S.-S. Ahn, C. D. Surh, S.-W. Yoon, D.-J. Kim, J. Choi, Y. Park, Y. C. Sung,

1013 and S.-W. Lee. 2015. Intranasal introduction of Fc-fused interleukin-7

1014 provides long-lasting prophylaxis from lethal influenza infection. *J. Virol.* 90:

1015 2273–2284.

1016 72. Foss, S., A. Grevys, K. M. K. Sand, M. Bern, P. Blundell, T. E.

1017 Michaelsen, R. J. Pleass, I. Sandlie, and J. T. Andersen. 2016. Enhanced

1018 FcRn-dependent transepithelial delivery of IgG by Fc-engineering and

1019 polymerization. *J. Control. Release* 223: 43–52.

1020 73. Sockolosky, J. T., and F. C. Szoka. 2015. The neonatal Fc receptor,

FcRn, as a target for drug delivery and therapy. *Adv. Drug Deliv. Rev.* 91: 109–124.

74. Patton, J. S., and P. R. Byron. 2007. Inhaling medicines: Delivering drugs to the body through the lungs. *Nat. Rev. Drug Discov.* 6: 67–74.

75. Heise, T., C. Büll, D. M. Beurskens, E. Rossing, M. I. De Jonge, G. J. Adema, T. J. Boltje, and J. D. Langereis. 2017. Metabolic Oligosaccharide Engineering with Alkyne Sialic Acids Confers Neuraminidase Resistance and Inhibits Influenza Reproduction. *Bioconjug. Chem.* 28: 1811–1815.

76. Niezold, T., M. Storcksdieck genannt Bonsmann, A. Maaske, V. Temchura, V. Heinecke, D. Hannaman, J. Buer, C. Ehrhardt, W. Hansen, K. Überla, and M. Tenbusch. 2015. DNA vaccines encoding DEC205-targeted antigens: Immunity or tolerance? *Immunology* 145: 519–533.

77. Jiang, W., W. J. Swiggard, C. Heufler, M. Peng, A. Mirza, R. M. Steinman, and M. C. Nussenzweig. 1995. The receptor DEC-205 expressed by dendritic cells and thymic epithelial cells is involved in antigen processing. *Nature* 375: 151–155.

78. Coconi-Linares, N., E. Ortega-Dávila, M. López-González, J. García-Machorro, J. García-Cordero, R. M. Steinman, L. Cedillo-Barrón, and M. A. Gómez-Lim. 2013. Targeting of envelope domain III protein of DENV type 2 to DEC-205 receptor elicits neutralizing antibodies in mice. *Vaccine* 31: 2366–2371.

79. Nesspor, T. C., T. S. Raju, C. N. Chin, O. Vafa, and R. J. Brezski. 2012. Avidity confers FcγR binding and immune effector function to aglycosylated immunoglobulin G1. *J. Mol. Recognit.* 25: 147–154.

80. Wines, B. D., H. A. Vanderven, S. E. Esparon, A. B. Kristensen, S. J. Kent, and P. M. Hogarth. 2016. Dimeric FcγR Ectodomains as Probes of the Fc Receptor Function of Anti-Influenza Virus IgG. *J. Immunol.* 197: 1507–1516.

81. Bournazos, S., and J. V. Ravetch. 2017. Fcγ Receptor Function and the Design of Vaccination Strategies. *Immunity* 47: 224–233.

82. Chang, Y., and V. Nizet. 2014. The interplay between Siglecs and sialylated pathogens. *Glycobiology* 24: 818-825.

Table 1. Summary of mutants and their interactions with glycan receptors.

Table 2. Summary of mutants and their interactions with Fcγ-receptors.

Table 3. Summary of mutants and their interactions with complement and influenza hemagglutinin.

Legends

FIGURE 1. Schematic showing the various hexa-Fc glycan mutants in which Cys^{575} is mutated to alanine to create the C575A panel of mutants. Red stars indicate the hinge Asn^{221}, the Cγ2 Asn^{297}, and the tailpiece Asn^{563} glycan sites.

 FIGURE 2. Schematic showing the C575A panel of glycan mutants from Fig. 1 in which the which Cys^{309} and Leucine^{310} is additionally changed to leucine and histidine as found in the native IgG1 Fc sequence to create the C309L/C575A panel of mutants. Red stars indicate the hinge Asn^{221}, the Cγ2 Asn^{297}, and the tailpiece Asn^{563} glycan sites.

FIGURE 3. Characterization of mutant Fc proteins by SDS-PAGE. (**A**) N563A/C575A, N297A/N563A/C575A form laddered multimers (red arrows) with folding intermediates (blue arrows) that are different to those formed by the hexa-Fc control. The C575A and N297A/C575A mutants run as monomers, with dimers and trimers also seen. Removal of Asn^{563} favors multimerization in the presence of Cys^{309} but the absence of Cys^{575}. The addition of a N-X-(T/S) glycan sequon to generate N-terminally glycosylated hinges (the D221N series of mutants) did not affect multimerization but increased the molecular mass of all mutants. (**B**) the same mutants as in panel A but run under reducing conditions. (**C**) the same mutants as in panel A but stained with Coomassie reagent. The decreasing molecular masses seen in the Fc represent sequential loss of N-linked glycans. The

1088 N297A/N563A/C575A mutant has the smallest molecular mass because it has

1089 no glycans attached to the Fc, and D221N/C575A has the largest mass

1090 because it has three glycans attached. The types of glycans attached at

1091 Asn[221], Asn[297] and Asn[563] for all mutants are shown in Supplemental Fig. S2-

1092 S4. (**D**) Substitution of Cys[309] with leucine onto the mutants shown in panel A

1093 to create the double cysteine knockouts, which run as monomers. Differing

1094 molecular masses are seen with C309L/N297A/C575A monomers, which may

1095 represent differential glycosylation of Asn[563]. (**E**) the same mutants as in panel

1096 D but run under reducing conditions. (**F**) Coomassie-stained gel of panel D.

1097 All proteins were run under either non-reducing or reducing conditions at 2 μg

1098 protein per lane on a 4-8% acrylamide gradient gel, transferred to

1099 nitrocellulose, and blotted with anti-human IgG Fc (Sigma).

1100

1101 **FIGURE 4**. Binding of the C309L and C575A double cysteine IgG1-Fc

1102 glycosylation mutants to glycan receptors. Mutants lacking either the N297

1103 and/or N563 glycans are severely restricted in their capacity to bind glycan

1104 receptors as determined by ELISA. The addition of an N-linked sugar at

1105 position 221 into the Asn[297] and/or Asn[563] mutants reinstates binding to all

1106 receptors investigated, with the exception of MBL, MMR and DC-SIGN.

1107 Insertion of Asn[221] into C309L/C575A enhances interactions to all the glycan

1108 receptors investigated. Error bars represent standard deviations around the

1109 mean value, n=2 independent experiments.

1110

1111 **FIGURE 5.** Binding of C575A mutants to glycan receptors. Proteins with a

1112 predisposition to multimerize via Cys[309] interactions (as shown in Fig. 3A, 3C

1113 and Supplemental Fig. S1C) are less able to engage glycan receptors than

1114 their equivalent mutants in which Cys[309] was changed to leucine (Fig. 3D, 3F).

1115 With the exception of Siglec-1, the insertion of Asn[221] into mutants that tend to

1116 form multimers had no effect on, or was detrimental to, binding of glycan

1117 receptors. Error bars represent standard deviations around the mean value,

1118 n=2 independent experiments.

1119

1120

1121 **FIGURE 6.** Binding of C309L (panels A-C) and the C575A (panels D-F)

1122 glycosylation mutants to classical FcγRs. The D221N/C309L/N563A/C575A

1123 mutant shows enhanced binding to FcγRI, FcγRIIB and FcγRIIIA, while

1124 C309L/N563A/C575A only shows enhanced binding to FcγRI and FcγRIIIA.

1125 Mutant N563A/C575A with a predisposition to multimerize via Cys[309]

1126 interactions (as shown in Fig. 3A,3C) binds strongly to FcγRI and FcγRIIIA as

1127 is also seen with C309L/N563A/C575A that carry the same N563A mutation.

1128 The D221N/N563A/C575A mutant shows enhanced binding to FcγRI and

1129 FcγRIIIA. In multimers the presence of Asn[221] constrains interactions with

1130 FcγRIIB that are enhanced when Asn[221] is attached to monomers (panel E).

1131 No improvement in binding was observed to FcγRIIA or FcγRIIIB for any of the

1132 mutants tested (data not shown). Error bars represent standard deviations

1133 around the mean value, n=2 independent experiments.

1134

1135 **FIGURE 7.** Binding of selected mutants to FcγRs by Biacore SPR analysis.

1136 (**A**) Binding of C309L/N297A/C575A, D221N/C309L/N297A/C575A,

1137 C309L/N563A/C575A, D221N/C309L/N563A/C575A, and monomeric Fc

1138 control to human FcγRI (CD64). Curves shown for molecules at 300nM,

1139 150nM and 75nM respectively. (**B**) Binding of the same mutants to FcγRIIIA-

1140 Val[176] (CD32A). Curves shown for molecules at 8000nM, 4000nM and

1141 2000nM respectively. Due to the varying stoichiometry of the molecules

1142 shown (Fig. 3 and Fig. S1C) an accurate determination of interaction kinetics

1143 is not possible. Binding to FcγRs from R&D systems is illustrated although

1144 binding with receptors sourced from Sino Biological gave nearly identical

1145 results.

1146

1147 **FIGURE 8.** Binding of the C309L and C575A mutants to complement. **(A)** Both

1148 the C309L/N563A/C575A and C309L/N297A/N563A/C575A mutants bound

1149 C1q and permitted C5b-9 deposition. Insertion of Asn[221] into both these mutants

1150 to create D221N/C309L/N563A/C575A and

1151 D221N/C309L/N297A/N563A/C575A allows C1q deposition but prevented

1152 subsequent C5b-9 deposition. This shows that the presence of the Asn[221]

1153 glycan, while allowing C1q to bind, blocks subsequent downstream activation of

1154 the classical pathway. Mutants in which only the Asn[297] glycan was removed, as
1155 in C309L/N297A/C575A or D221N/C309L/N297A/C575A were unable to bind
1156 C1q or fix C5b-9. (**B**) Binding of the C575A mutants to complement. With the
1157 exception of D221N/N563A/C575A, the presence of Asn[221] inhibited binding to
1158 C1q, although all Asn[221]-containing mutants including D221N/N563A/C575A
1159 were unable to fix C5b-9. Error bars represent standard deviations around the
1160 mean value, n=2 independent experiments.

1161

1162 **FIGURE 9.** MALDI-TOF MS profiles of permethylated N-glycans from
1163 N297A/C575A and D221N/N297A/N563A/C575A IgG1-Fc mutants. The data
1164 were acquired in the positive ion mode to observe [M + Na]+ molecular ions.
1165 All the structures are based on composition and knowledge of biosynthetic
1166 pathways. Structures shown outside a bracket have not had their antenna
1167 location unequivocally defined.

1168

1169 **FIGURE 10**. Impact of Fc glycosylation. (**A**) ELISA binding of the C309L/C575A
1170 panel and (**B**) the C575A panel of Fc glycosylation mutants to hemagglutinin.
1171 (**C**) impact of Fc glycosylation on hemagglutination inhibition. A constant
1172 amount of influenza A New Caledonia/20/99 virus H1N1 was incubated with
1173 titrated amounts of the Fc glycan mutants and added to human O$^+$ erythrocytes
1174 that were then allowed to sediment at room temperature for 1h. Non-
1175 agglutinated RBCs form a small halo. n=2 independent experiments.

1176

1177 **FIGURE 11.** Model showing proposed cis interactions of the tri-glycan
1178 D221N/C575A mutant with (**A**) glycan receptors or (**B**) influenza hemagglutinin.
1179 The glycan at Asn[297] in the wildtype IgG1 Fc is buried and unable to interact
1180 directly with receptors. However, monomers with glycans located at both the N-
1181 and C-terminii of the Fc (Asn[221] and Asn[563]), as in D221N/C575A, are exposed
1182 and therefore allow cross-linking of sialic acid-dependent receptors (including
1183 Siglec-1 or hemagglutinin) (50).

Footnotes

Figure 1

Fc-construct	Heavy chain composition	State by SDS-PAGE	State by SEC-HPLC
IgG1-Fc		monomer	monomer
Hexa-Fc		barrel	barrel
C575A		monomer >dimer >trimer	monomer >dimer
N297A/C575A		monomer >dimer >trimer	monomer >dimer
N563A/C575A		ladder	monomer multimer
N297A/N563A/C575A		ladder	multimer
D221N/C575A		monomer >dimer	monomer >dimer
D221N/N297A/C575A		monomer >dimer	monomer
D221N/N563A/C575A		ladder	multimer
D221N/N297A/N563A/C575A		ladder	multimer
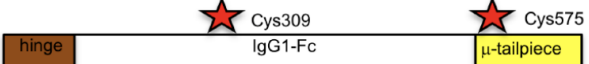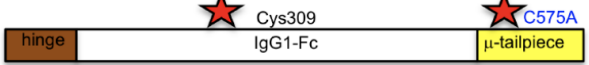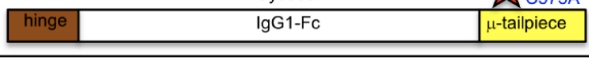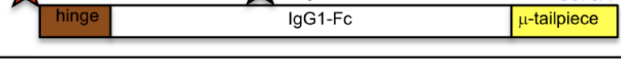
Figure 2

Fc-construct	Heavy chain composition	State by SDS-PAGE	State by SEC-HPLC
Hexa-Fc	hinge — IgG1-Fc — μ-tailpiece (Cys309, Cys575)	barrel	multimer
C309L	hinge — IgG1-Fc — μ-tailpiece (C309L, Cys575)	ladder	multimer
C309L/C575A	hinge — IgG1-Fc — μ-tailpiece (C309L, C575A)	monomer	monomer
C309L/N297A/C575A	hinge — IgG1-Fc — μ-tailpiece (C309L, C575A)	monomer	monomer
C309L/N563A/C575A	hinge — IgG1-Fc — μ-tailpiece (C309L, C575A)	monomer	multimer
C309L/N297A/N563A/C575A	hinge — IgG1-Fc — μ-tailpiece (C309L, C575A)	monomer	multimer
D221N/C309L/C575A	hinge — IgG1-Fc — μ-tailpiece (C309L, C575A)	monomer	monomer
D221N/C309L/N297A/C575A	hinge — IgG1-Fc — μ-tailpiece (C309L, C575A)	monomer	monomer
D221N/C309L/N563A/C575A	hinge — IgG1-Fc — μ-tailpiece (C309L, C575A)	monomer >dimer	multimer
D221N/C309L/N297A/N563A/C575A	hinge — IgG1-Fc — μ-tailpiece (C309L, C575A)	monomer	monomer multimer >dimer

Figure 3
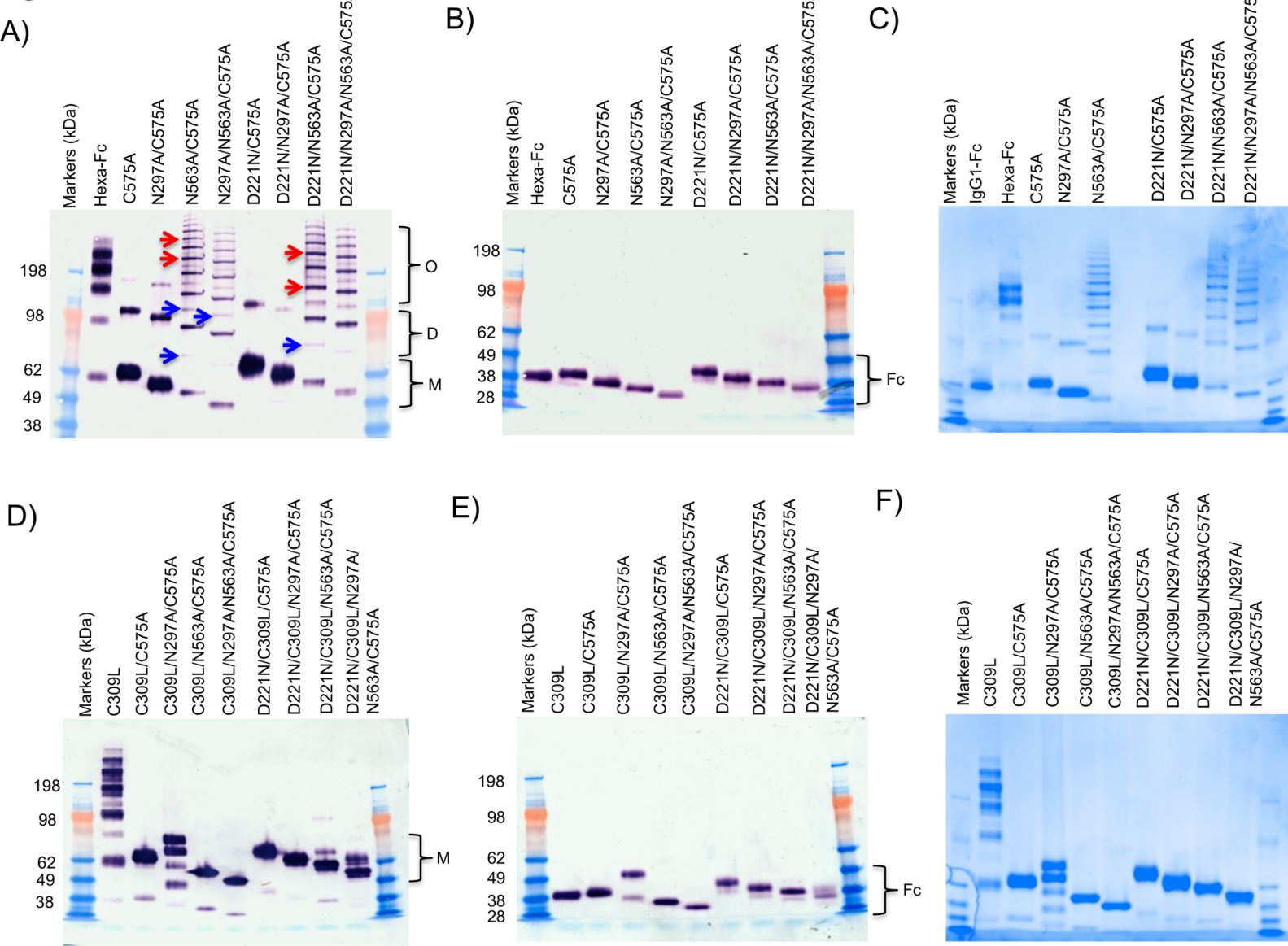
Figure 4
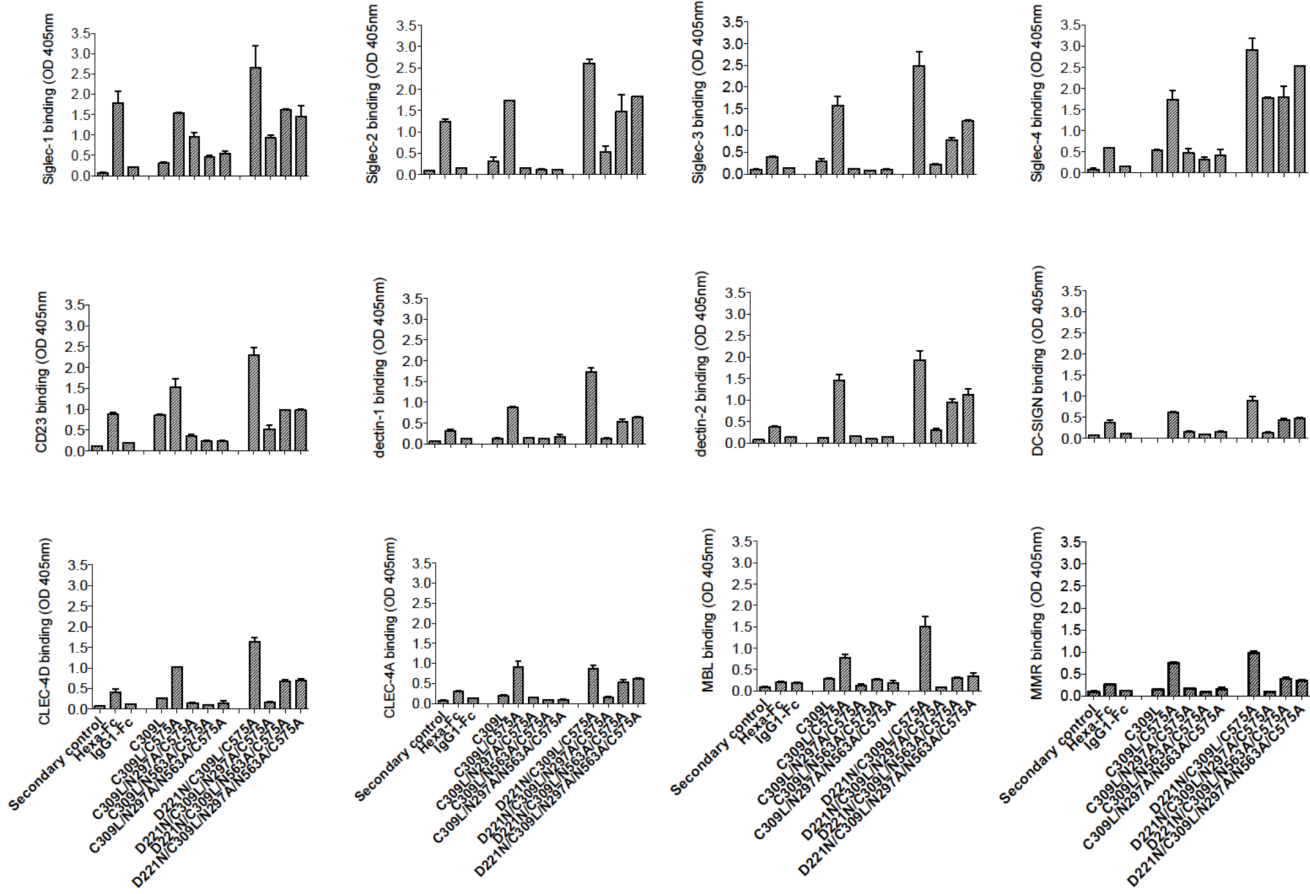
Figure 5

Figure 6

Figure 7

Figure 8

A)

C1q binding (OD 405nm)

C5b-9 binding (OD 405nm)

Fc (μg/ml)
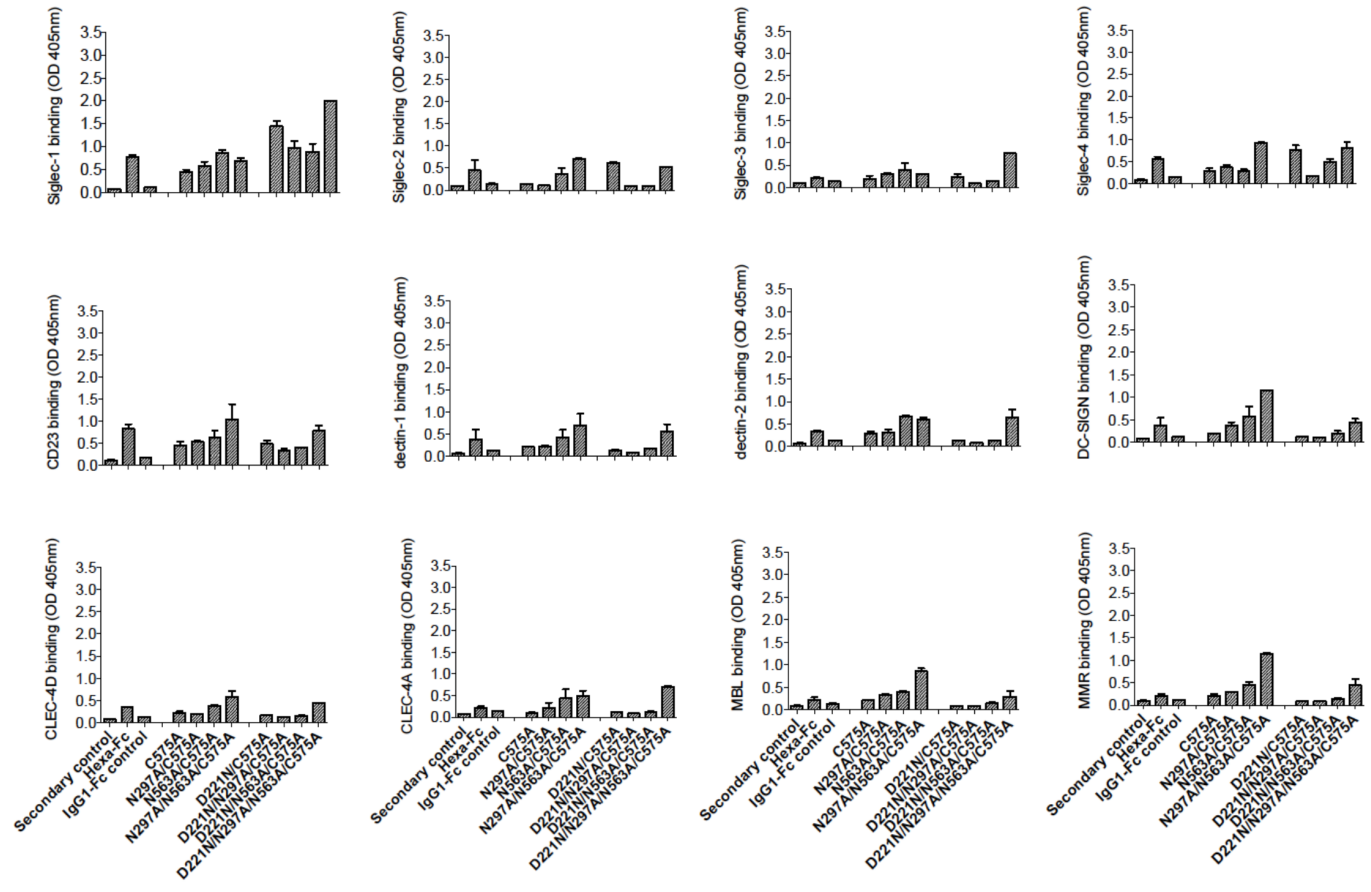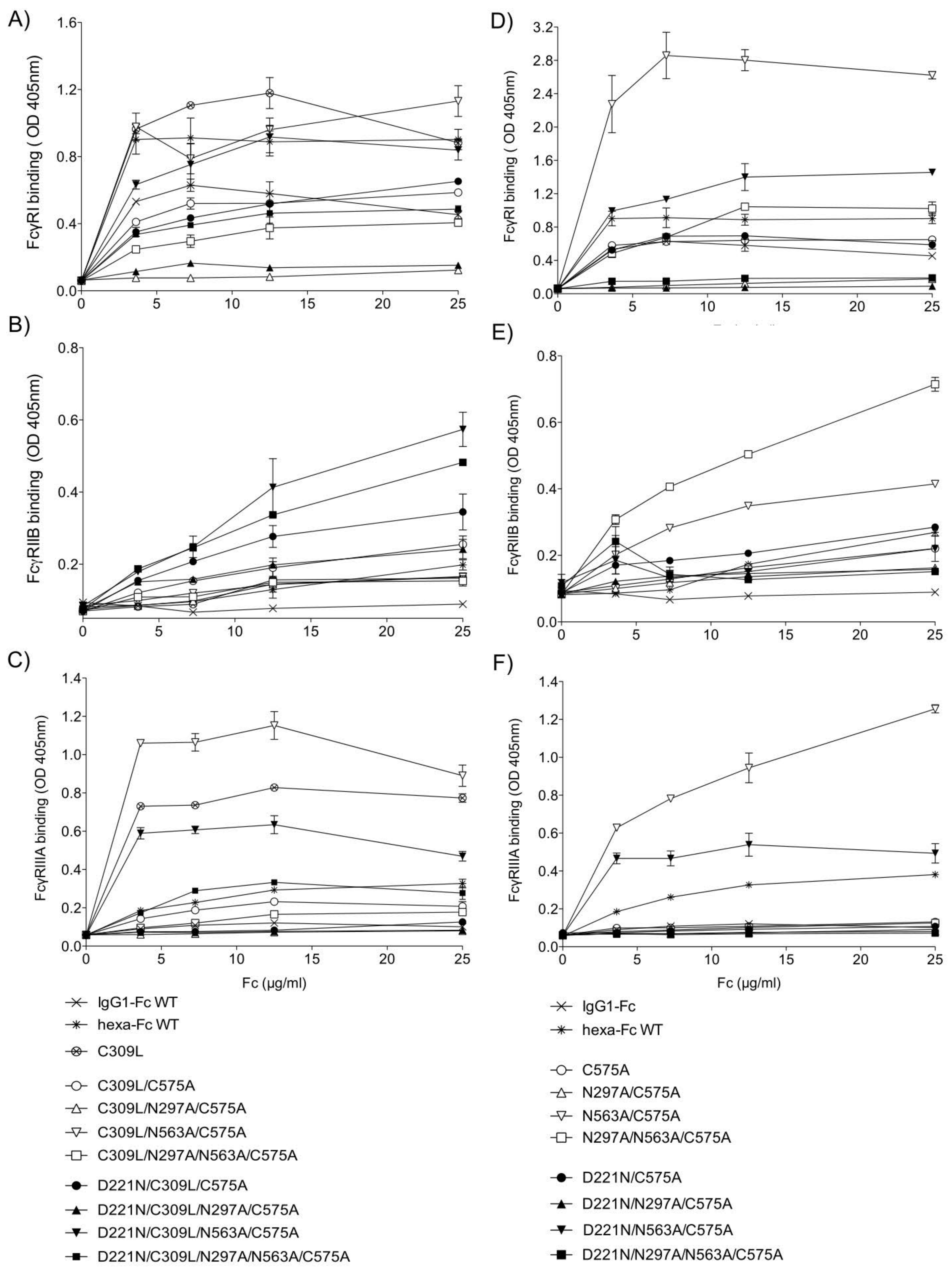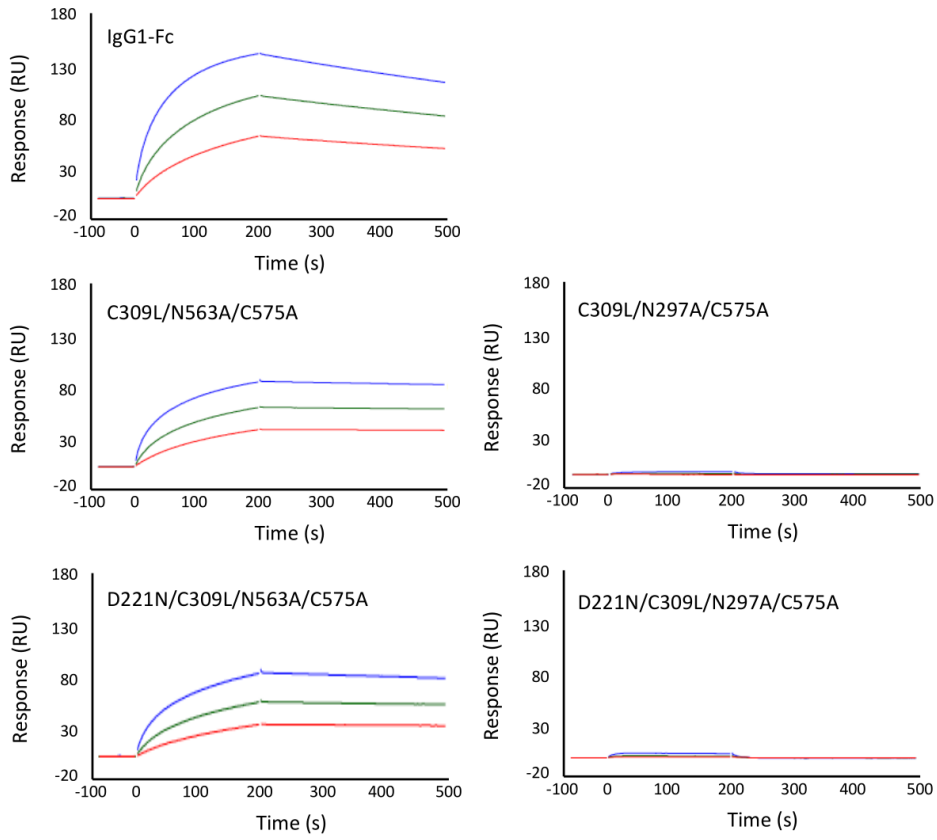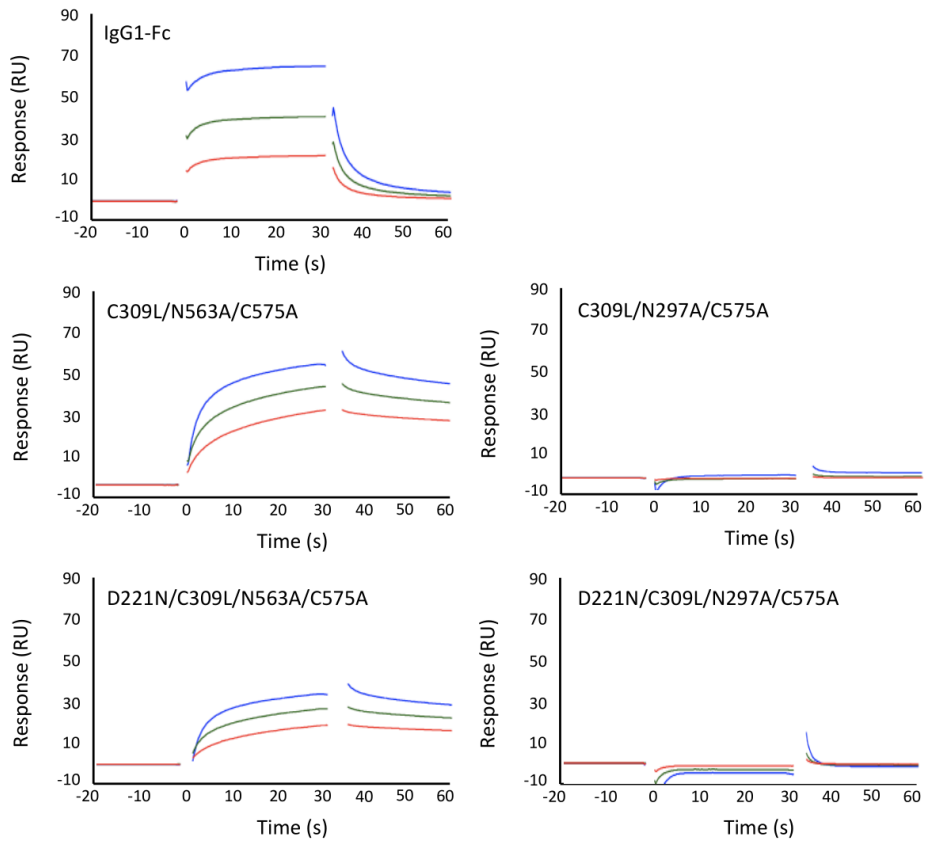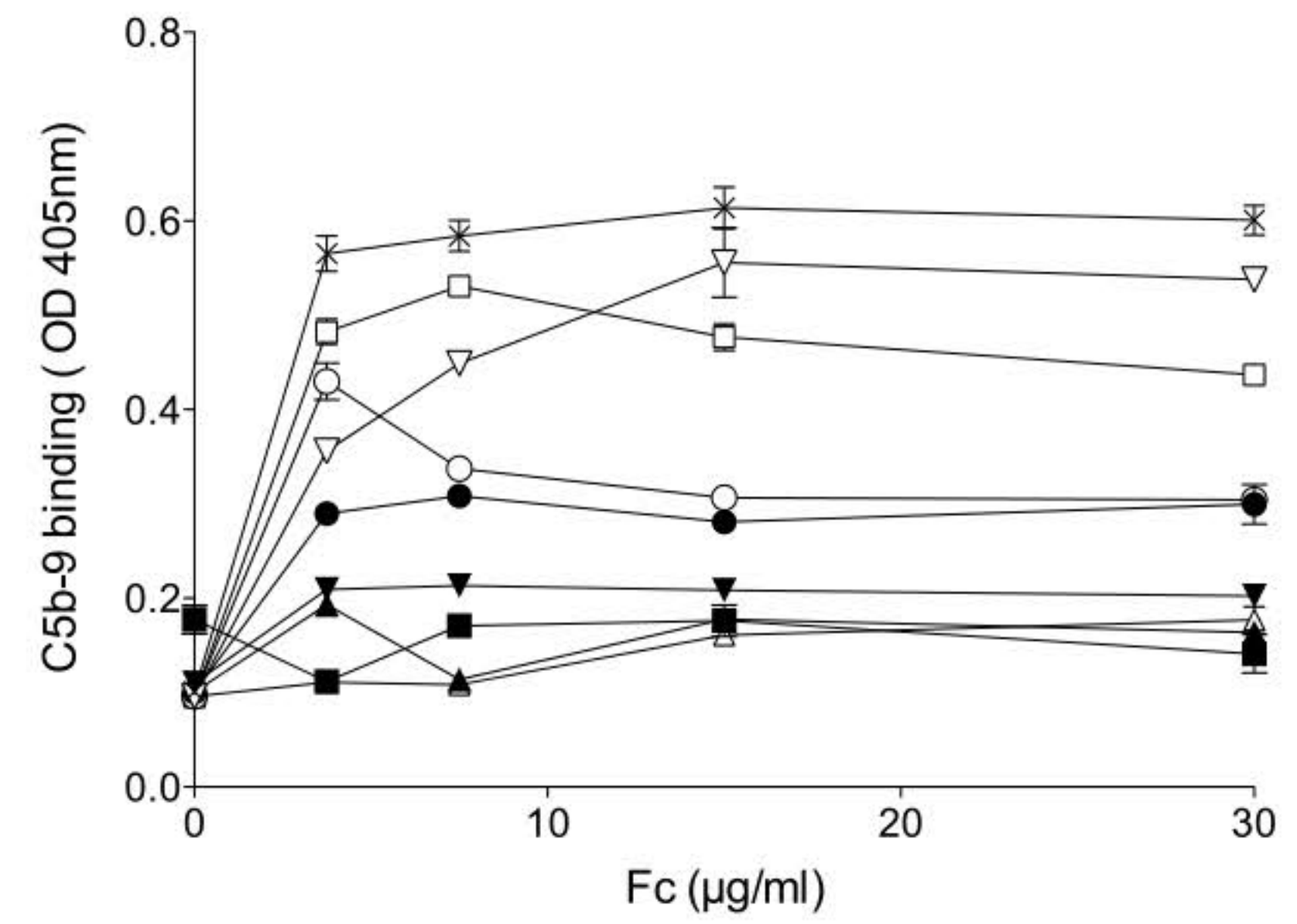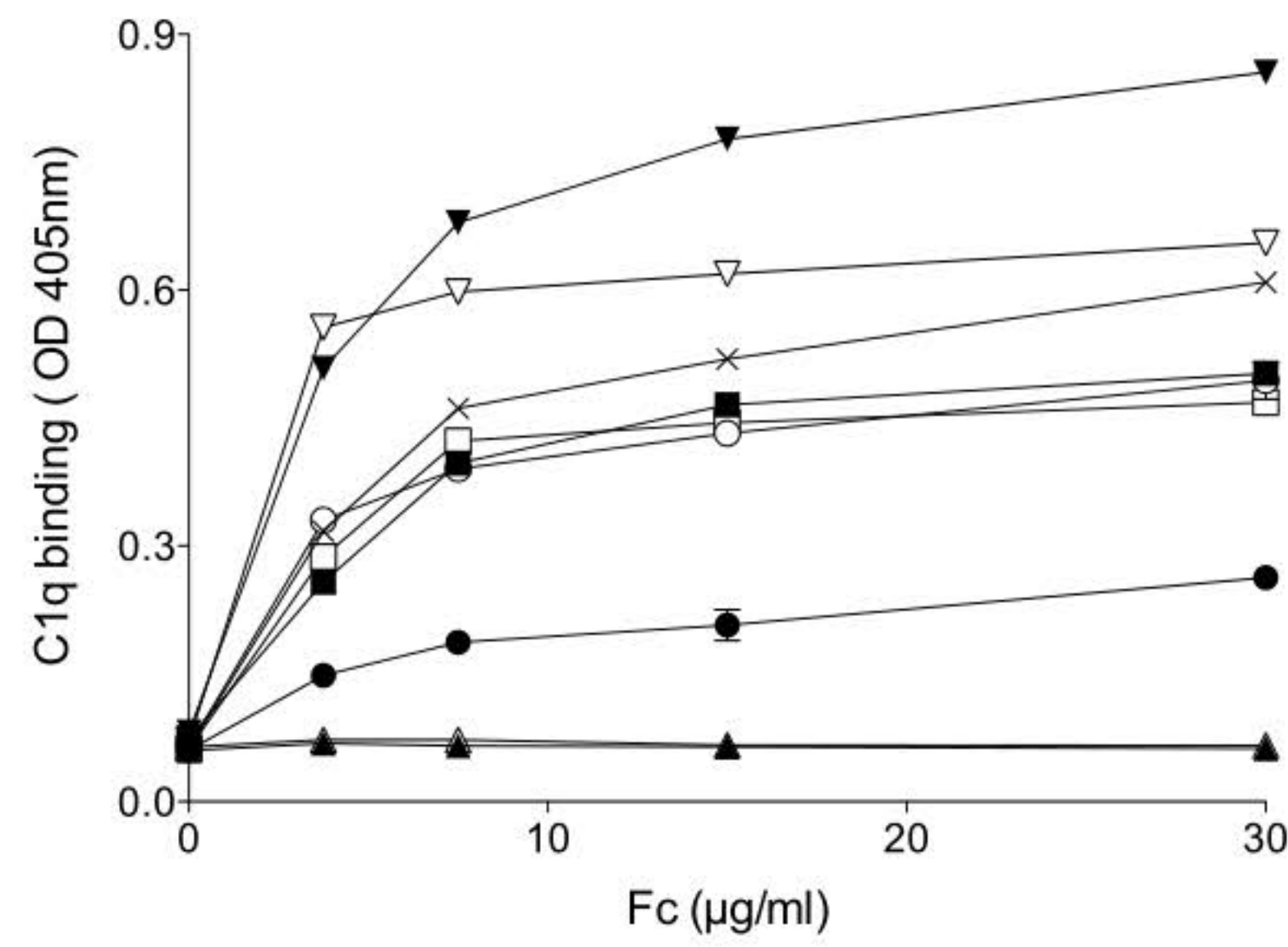
-✕- IgG1-Fc WT
-○- C309L/C575A
-△- C309L/N297A/C575A
-▽- C309L/N563A/C575A
-□- C309L/N297A/N563A/C575A
-●- D221N/C309L/C575A
-▲- D221N/C309L/N297A/C575A
-▼- D221N/C309L/N563A/C575A
-■- D221N/C309L/N297A/N563A/C575A

B)

C1q binding (OD 405nm)

C5b-9 binding (OD 405nm)

Fc (μg/ml)
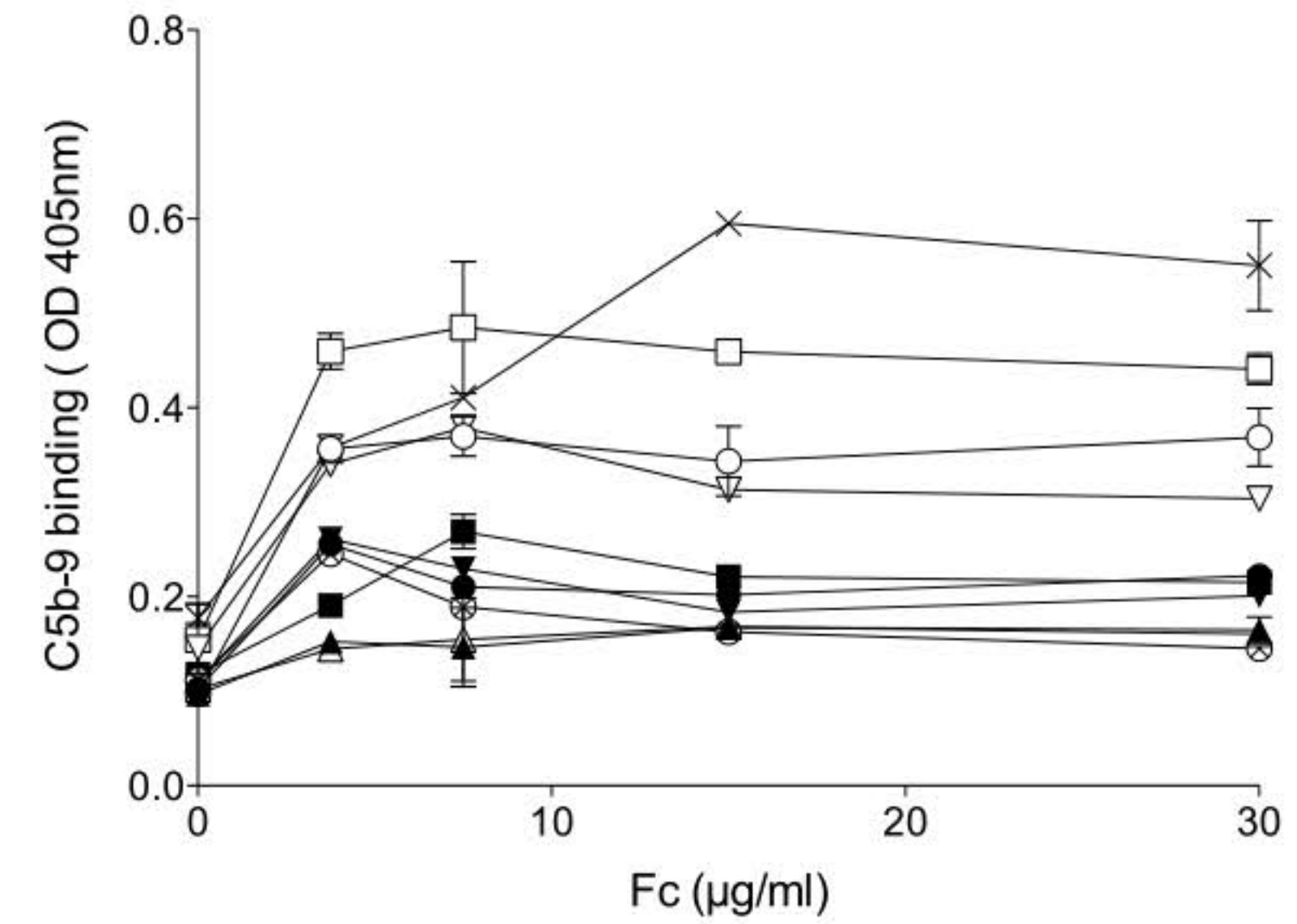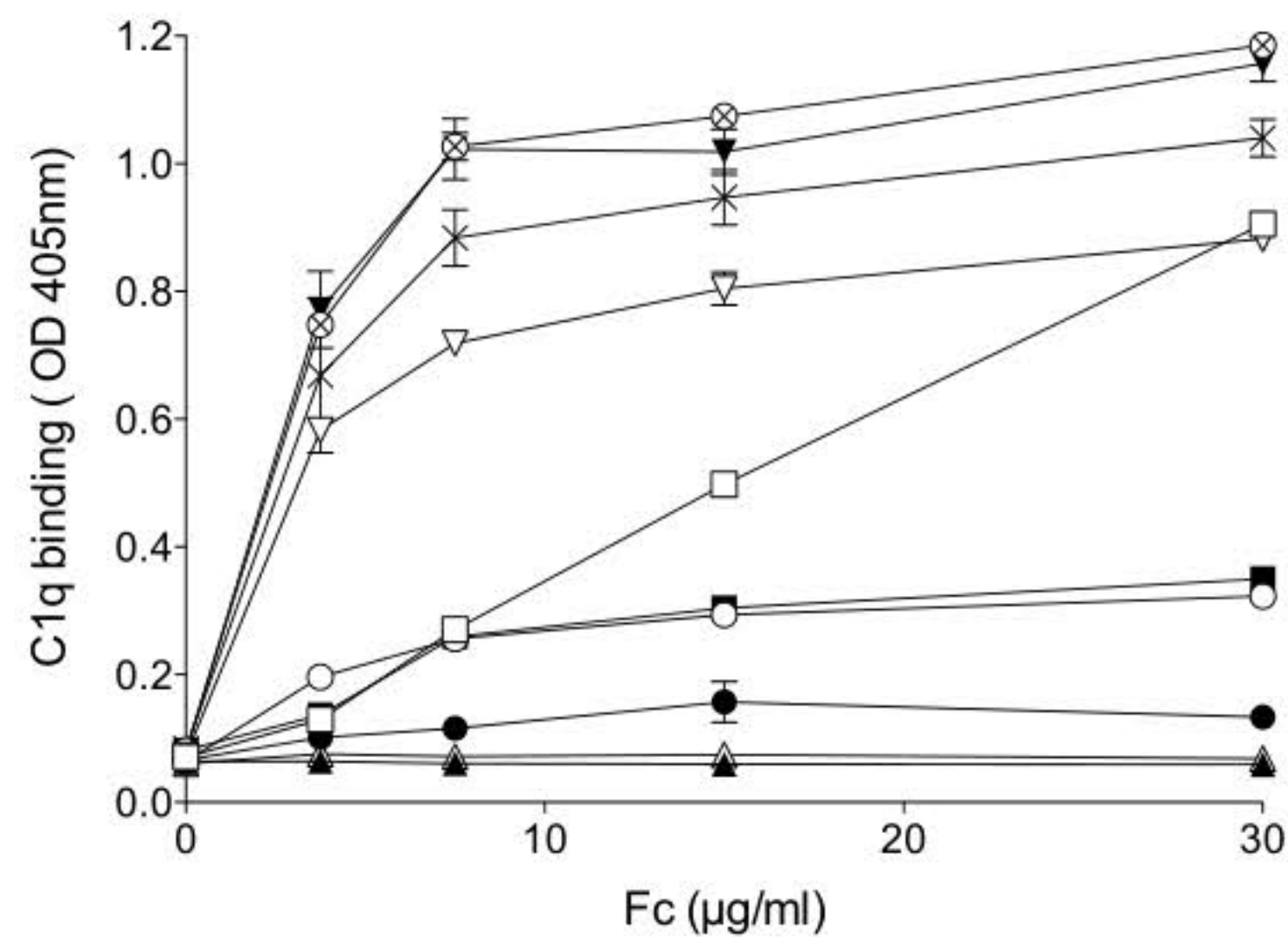
-✕- hexa-Fc WT
-⊗- C309L
-○- C575A
-△- N297A/C575A
-▽- N563A/C575A
-□- N297A/N563A/C575A
-●- D221N/C575A
-▲- D221N/N297A/C575A
-▼- D221N/N563A/C575A
-■- D221N/N297A/N563A/C575A

Figure 9

Figure 10

A)

B)

C)
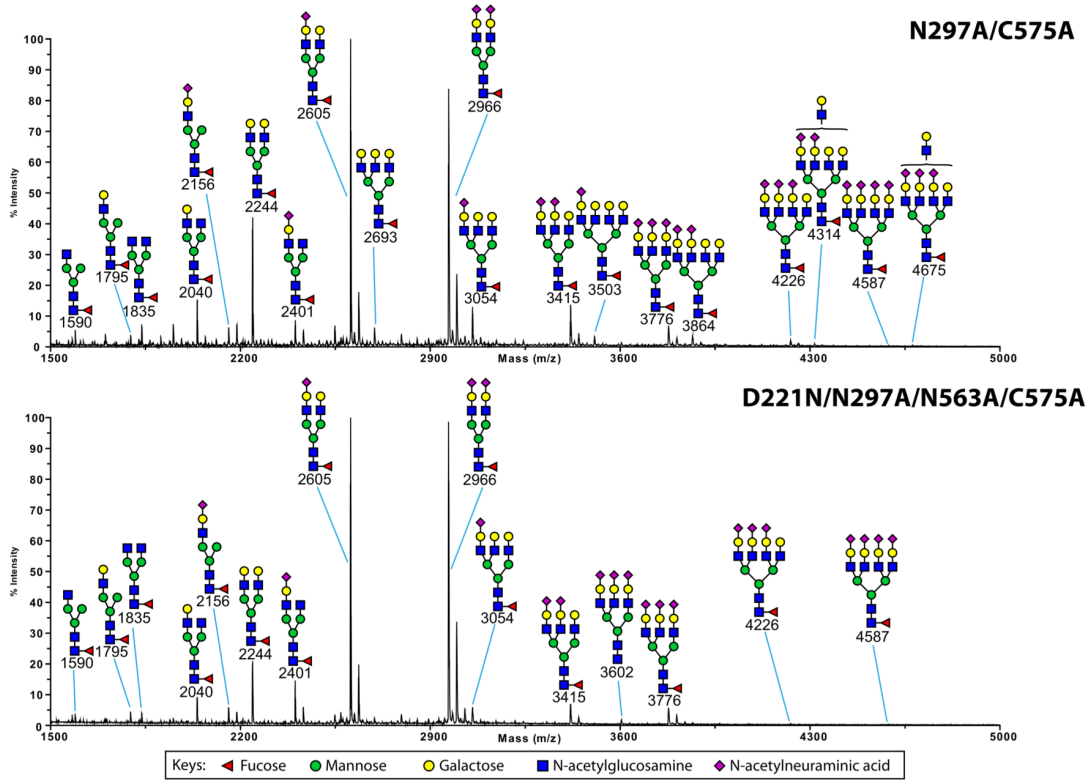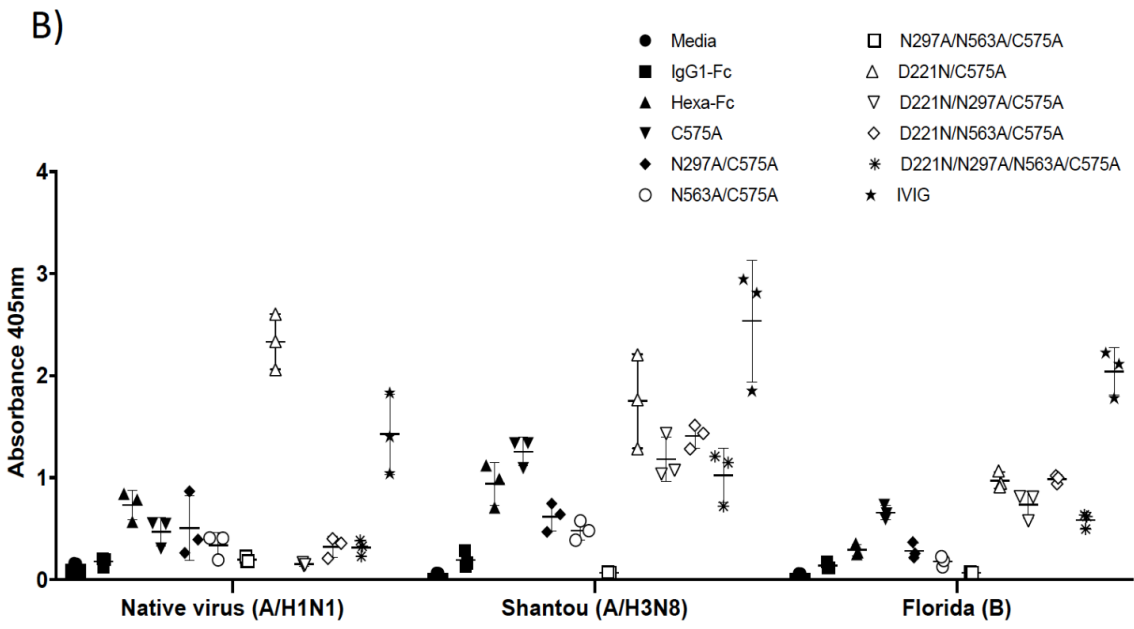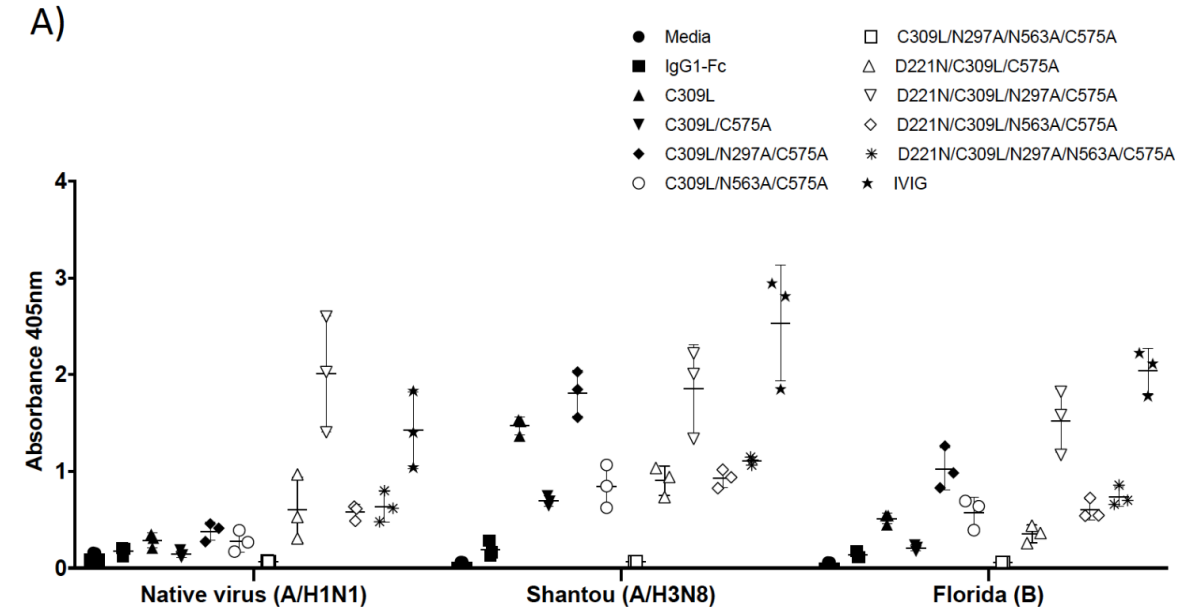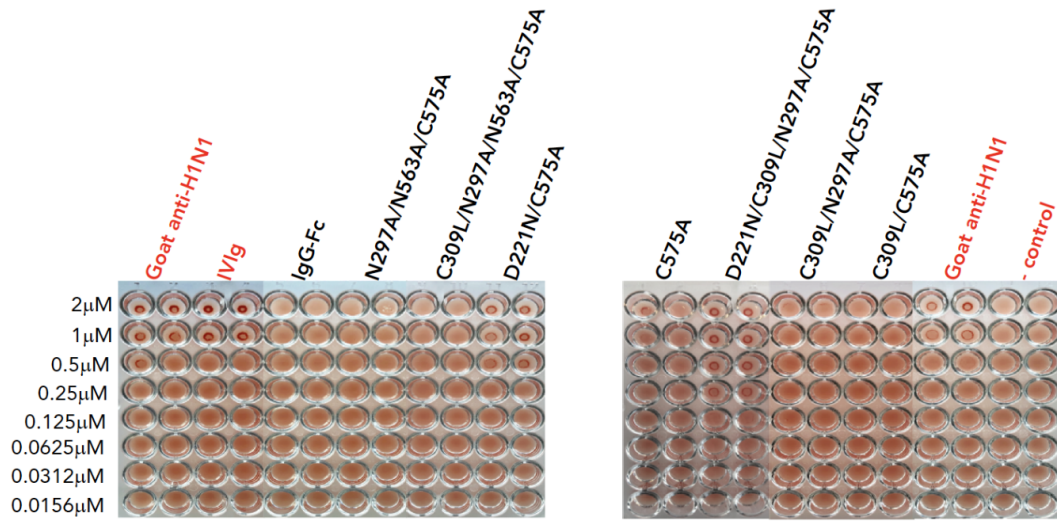
Figure 11
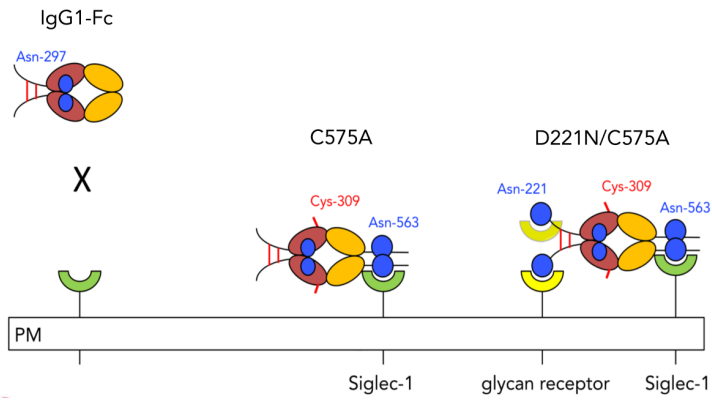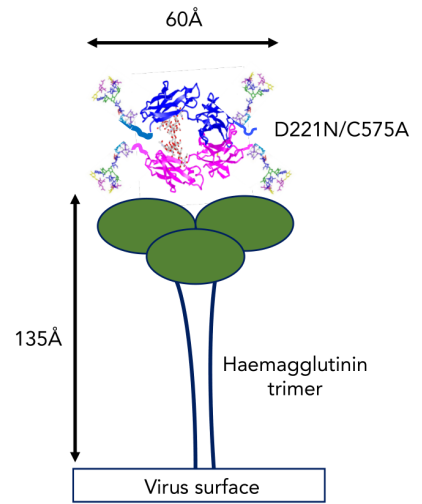
Glycan receptors	Complex sialylated glycans detected	Siglec-1	Siglec-2	Siglec-3	Siglec-4	CD23	dectin-1	dectin-2	DC-SIGN	clec-4A	clec-4D	MBL	MMR	DEC-205
C309L/N297A/N563A/C575A	-	-	-	-	-	-	-	-	-	-	-	-	-	-
IgG1-Fc	-	-	-	-	-	-	-	-	-	-	-	-	IgG1-Fc	nd
N297A/C575A	+	+	-	-	-	-/+	-	-	-	-	-	-	-	-	nd
D221N/N297A/C575A	+++	++	-	-	-	-/+	-	-	-	-	-	-	-	-	nd
C309L/N297A/C575A	+++	++	-	-	-/+	-	-	-	-	-	-	-	-	-	nd
D221N/C309L/N297A/C575A	+++	++	-/+	-	+++	-/+	-	-	-	-	-	-	-	-	nd
C575A	-/+	+	-	-	-	-/+	-	-	-	-	-	-	-	-	nd
D221N/C575A	+++	++	+	-	+	-/+	-	-	-	-	-	-	-	-	nd
C309L/C575A	-/+	+++	+++	+++	+++	+++	++	++	+	+	+	+	+	+++
D221N/C309L/C575A	+	++++	++++	++++	++++	++++	+++	+++	+	++	+	+++	+++	+++
C309L/N563A/C575A	-	-	-	-	-/+	-	-	-	-	-	-	-	-	-	nd
D221N/C309L/N297A/N563A/C575A	++	++	+++	++	+++	+	+	++	-/+	+	-/+	-	-	++++
D221N/C309L/N563A/C575A	+	++	+++	+	+++	+	+	+	-/+	+	-/+	-	-	nd
D221N/N297A/N563A/C575A	+++	++	-/+	+	+	+	-	-/+	-	-	+	-	-	nd
Hexa-Fc	+	++	++	-	-/+	+	-	-	+	-	-	-	-	+
D221N/N563A/C575A	+	+	-	-	-/+	-	-	-/+	-	-	-	-	-	nd
C309L	++	-	-	-	-	+	-	-	-	-	-	-	-	-
N297A/N563A/C575A	-	+	+	-	+	-	-/+	-/+	+	-	-	+	++	nd
N563A/C575A	-/+	++	-/+	-	-	-	-/+	-/+	-/+	-/+	-	-	-	nd

Table 1. Summary of mutants and their interactions with glycan receptors.

Fcγ-receptors	Complex sialylated glycans detected		FcγRI	FcγRIIA	FcγRIIB	FcγRIIIA	FcγRIIIB
C309L/N297A/N563A/C575A	-		-	-	-	-	-
IgG1-Fc	-		+	-	-	-	-
N297A/C575A	+		-	-	-	-	-
D221N/N297A/C575A	+++		-	-	-	-	-
C309L/N297A/C575A	+++		-	-	-	-	-
D221N/C309L/N297A/C575A	+++		-	-	-	-	-
C575A	-/+		+	-	-	-	-
D221N/C575A	+++		+	-	-/+	-	-
C309L/C575A	-/+		+	-	-	-	-
D221N/C309L/C575A	+		+	-	+	-	-
C309L/N563A/C575A	-		++	-	-	+++	-
D221N/C309L/N297A/N563A/C575A	++		+	-	++	-/+	-
D221N/C309L/N563A/C575A	+		++	-	+++	++	-
D221N/N297A/N563A/C575A	+++		-	-	-	-	-
Hexa-Fc	+		++	+	-/+	+	-
D221N/N563A/C575A	+		++	-	-	++	-
C309L	++		++	-	-	+++	-
N297A/N563A/C575A	-		++	-	+++	-	-
N563A/C575A	-/+		++++	-	+	++++	-

Table 2. Summary of mutants and their interactions with Fcγ-receptors.

	Complex sialylated glycans detected		C1q	C5b-9	Binds Native Influenza virus (Caledonia A/H1N1)	Binds Recombinant HA (Shantou A/H3N8)	Binds Recombinant HA (Florida B)	Inhibits Influenza Virus (Caledonia A/H1N1) agglutination
C309L/N297A/N563A/C575A	-		+	+	-	-	-	No
IgG1-Fc	-		+	+	-	-	-	No
N297A/C575A	+		-	-	-	-/+	-	n.d.
D221N/N297A/C575A	+++		-	-	-	++	+	n.d.
C309L/N297A/C575A	+++		-	-	-	+++	++	No
D221N/C309L/N297A/C575A	+++		-	-	++++	+++	+++	Yes
C575A	-/+		--/+	-/+	-	++	+	No
D221N/C575A	+++		-	-	++++	+++	++	Yes
C309L/C575A	-/+		+	-/+	-	+	-	No
D221N/C309L/C575A	+		--/+	-/+	+	+	-	n.d.
C309L/N563A/C575A	-		++	+	-	+	-	n.d.
D221N/C309L/N297A/N563A/C575A	++		+	-	+	++	+	n.d.
D221N/C309L/N563A/C575A	+		++	-	+	++	+	n.d.
D221N/N297A/N563A/C575A	+++		--/+	-	-	+	-/+	n.d.
Hexa-Fc	+		+++	+	+	+	-	n.d.
D221N/N563A/C575A	+		+++	-	-	++	+	n.d.
C309L	++		+++	-	-	++	-/+	n.d.
N297A/N563A/C575A	-		+	+	-	-	-	No
N563A/C575A	-/+		++	-/+	-	-	-	n.d.

Table 3. Summary of mutants and their interactions with complement and influenza hemagglutinin.